

Towards a Theoretical Understanding of Batch Normalization

Jonas Kohler^{*1}, Hadi Daneshmand^{*1}, Aurelien Lucchi¹,
 Ming Zhou², Klaus Neymeyr², Thomas Hofmann¹ †
¹ Department of Computer Science, ETH Zurich
² Institute of Mathematics, University of Rostock

May 11, 2022

Abstract

Normalization techniques such as Batch Normalization have been applied very successfully for training deep neural networks. Yet, despite its apparent empirical benefits, the reasons behind the success of Batch Normalization are mostly hypothetical. We thus aim to provide a more thorough theoretical understanding from an optimization perspective. Our main contribution towards this goal is the identification of various problem instances in the realm of machine learning where, under certain assumptions, Batch Normalization can provably accelerate optimization with gradient-based methods. We thereby turn Batch Normalization from an effective practical heuristic into a provably converging algorithm for these settings. Furthermore, we substantiate our analysis with empirical evidence that suggests the validity of our theoretical results in a broader context.

1 Introduction

One of the most important recent innovations for optimizing deep neural networks is Batch Normalization (BN) [14]. This technique has proved to successfully stabilize and accelerate training of deep neural network and is thus by now standard in many state-of-the art architectures such as ResNets [13] and the latest Inception Nets [30]. The problem addressed by Batch Normalization is the well-known phenomenon of vanishing or exploding gradients that can make training unstable and cause divergence. The root of this problem lies in the use of deep models that involve the composition of nested functions which allows for rich modelling capacity but also creates complex dependencies between the individual parameters. Training such models involves computing gradients as a product of multiple Jacobian matrices which can quickly become unstable if the spectrum of the individual Jacobians is not within an appropriate range. It therefore seems natural that normalizing the inner layers of a neural network might stabilize training which recently led to the development of many such normalization methods such as [2, 3, 15, 27] to name just a few.

Despite the key role of Batch Normalization for training deep networks, the community is mostly relying on empirical evidence, lacking a thorough theoretical understanding explaining such success.

^{*}The first two authors have contributed equally in this work

[†]Correspondence to: Hadi Daneshmand (hadi.daneshmand@inf.ethz.ch)

Indeed, to the best of our knowledge, there exists no theoretical result which provably shows faster convergence rates for this technique on any problem instance.

Internal Covariate Shift The most widespread idea is that Batch Normalization accelerates training by reducing the so-called *covariate shift*, defined as the change in the distribution of inputs while the conditional distribution of outputs is unchanged. The problem of covariate shift can be even more severe for deep neural networks where the successive composition of layers drives the activation distribution away from the initial input distribution. It is argued that Batch Normalization reduces the internal covariate shift by employing a normalization technique that enforces the input distribution of each activation layer to be whitened - i.e. enforced to have zero means and unit variances - and decorrelated [14]. In a recent study, [28] provides evidence that questions the effectiveness of internal covariate shift in the performance of batch normalization.

Length-direction decoupling A different perspective was brought up recently by another normalization technique termed Weight Normalization (WN) [27]. This technique performs a normalization that is independent of any data statistics with the goal of decoupling the length of the weight vector from its direction. The optimization of the training objective is then performed by training the two parts separately. As discussed in Section 2, the two approaches differ in how the weights are normalized but share the above mentioned decoupling effect. Interestingly, weight normalization has been shown empirically to benefit from similar acceleration properties as Batch Normalization [11, 27]. This raises the obvious question whether or not reducing the internal covariate shift is the only explanation of the empirical gains observed when training with Batch Normalization techniques or whether part of its success can be attributed to the length-direction decoupling.

Our contribution We contribute a better theoretical understanding of Batch Normalization by analyzing it from an optimization perspective. In this regard, we particularly address the following question:

Can we find a setting in which Batch Normalization provably accelerates optimization with gradient-based methods and does the length-direction decoupling play a role in this phenomenon?

We answer both questions affirmatively. In particular, we show that the specific variance transformation of BN together with the length-direction decoupling allows local search methods to exploit certain global properties of the optimization landscape by leveraging an adaptive stepsize scheme. In this way, we obtain a *linear* convergence rate for a BN variant on the (possibly) non-convex problem of learning halfspaces with Gaussian inputs, which is a prominent problem in machine learning [10]. We thereby turn BN from an effective practical heuristic into a provably converging algorithm. Additionally we show that this technique can be considered as a non-linear reparametrization of the weight space, which can be very beneficial even for simple convex optimization tasks, such as logistic regressions. Interestingly, this fact that has received little to no attention within the optimization community (see [23] for an exception). Finally, we analyze the effect of BN while training a multilayer neural network (MLP) and prove – again under a similar Gaussianity assumption – that BN acts in such a way that the cross dependencies between layers are reduced and thus the curvature structure is simplified. Due to this dependency reduction, gradient-based optimization with an adaptive stepsize policy can enjoy a linear convergence rate on each individual unit. We substantiate both findings with experimental results on real world

datasets that confirm the validity of our analysis, despite certain theoretical assumptions that may not always hold in practice.

2 Background

Data distribution Suppose that $\mathbf{x} \in \mathbb{R}^d$ is a random input vector and $y \in \{\pm 1\}$ is the corresponding output variable. Throughout this paper we recurrently use the following statistics:

$$\mathbf{u} := \mathbf{E}[-y\mathbf{x}], \quad \mathbf{S} := \mathbf{E}[\mathbf{x}\mathbf{x}^\top], \quad (1)$$

and generally make the following (weak) assumption.

Assumption 1. *[Weak assumption on data distribution] We assume that $\mathbf{E}[\mathbf{x}] = 0$. We further assume that the spectrum of the matrix \mathbf{S} is bounded as*

$$0 < \mu := \lambda_{\min}(\mathbf{S}), L := \lambda_{\max}(\mathbf{S}) < \infty. \quad (2)$$

As a result, \mathbf{S} is the symmetric positive definite covariance matrix of \mathbf{x} .

The part of our analysis presented in Section 4 and 5 relies on a stronger assumption on the data distribution. In this regard we consider the combined random variable $\mathbf{z} := -y\mathbf{x}$, whose mean vector and covariance matrix are \mathbf{u} and \mathbf{S} as defined above in Eq. (1).

Assumption 2. *[Normality assumption on data distribution] We assume that \mathbf{z} is a multivariate normal random variable distributed as $\mathbf{z} \sim \mathcal{N}(\mathbf{u}, \mathbf{S})$.*

Batch normalization as a reparameterization of the weight space Consider the following objective function that typically occurs when minimizing an expected risk,

$$\min_{\tilde{\mathbf{w}} \in \mathbb{R}^d} \left(f(\tilde{\mathbf{w}}) := \mathbf{E}_{\mathbf{x}, y} \left[\ell(\mathbf{x}^\top \tilde{\mathbf{w}}, y) \right] \right), \quad (3)$$

where $\ell : \mathbb{R} \times \mathbb{R} \rightarrow \mathbb{R}^+$ is a sufficiently smooth loss function. We introduce the \mathbf{S} -normalization of a given parameter vector $\tilde{\mathbf{w}} \in \mathbb{R}^d$ by splitting it into a directional and a length component as

$$\tilde{\mathbf{w}} := g \frac{\mathbf{w}}{(\mathbf{w}^\top \mathbf{S} \mathbf{w})^{1/2}}, \quad (4)$$

where \mathbf{w} accounts for the direction and g for the scaling of $\tilde{\mathbf{w}}$. In order to keep concise notations, we will often use the induced norm of the positive definite matrix \mathbf{S} as $\|\mathbf{w}\|_{\mathbf{S}} = (\mathbf{w}^\top \mathbf{S} \mathbf{w})^{1/2}$.

The above reparameterization is an abstraction of Batch Normalization, where - for the sake of analyzability - we omit the following details: (i) computing the variance over a *mini*-batch, (ii) centering the input $\mathbf{x}^\top \mathbf{w}$.¹ Note that Weight Normalization ([27]) is another instance of the above reparameterization, where \mathbf{S} is replaced by \mathbf{I} . In both cases, the objective becomes invariant to linear scaling of \mathbf{w} . From a geometry perspective, WN can be understood as optimization on the unit

¹This condition is naturally satisfied in Section 3 and 4 due to the assumption that \mathbf{x} is zero-mean. Yet, we also omit centering for the neural network analysis in Section 5. This is done for the sake of simplicity but note that [27] found that the centering aspect of BN yields no empirical improvements in terms of optimization.

sphere, while BN operates on the \mathbf{S} -sphere (ellipsoid) [7]. Applying this type of \mathbf{S} -normalization when optimizing (3) can be interpreted as optimizing an alternative problem of the following form

$$\min_{\mathbf{w} \in \mathbb{R}^d, g \in \mathbb{R}} \left(f(\mathbf{w}, g) := \mathbf{E}_{\mathbf{x}, y} \left[\ell \left(\mathbf{x}^\top g \mathbf{w} / \|\mathbf{w}\|_{\mathbf{S}}, y \right) \right] \right). \quad (5)$$

In the following, we identify settings where reparametrizing the weight space in such a non-linear way is advantageous from an optimization point of view.

3 Ordinary least squares

As a preparation for subsequent analyses, we start with the simple convex quadratic objective encountered when minimizing an ordinary least squares problem, namely

$$\min_{\tilde{\mathbf{w}} \in \mathbb{R}^d} f_{\text{LS}}(\tilde{\mathbf{w}}) := \mathbf{E}_{\mathbf{x}, y} \left[\left(y - \mathbf{x}^\top \tilde{\mathbf{w}} \right)^2 \right] \stackrel{\text{(A1)}}{=} 2\mathbf{u}^\top \tilde{\mathbf{w}} + \tilde{\mathbf{w}}^\top \mathbf{S} \tilde{\mathbf{w}}. \quad (6)$$

When reparametrizing $\tilde{\mathbf{w}}$ according to (4), the above objective turns into the *non-convex* problem

$$\min_{\mathbf{w} \in \mathbb{R}^d, g \in \mathbb{R}} \left(f_{\text{LS}}(\mathbf{w}, g) := 2g \frac{\mathbf{u}^\top \mathbf{w}}{\|\mathbf{w}\|_{\mathbf{S}}} + g^2 \right). \quad (7)$$

Despite the non-convexity of this new objective, we will prove that gradient descent (GD) enjoys a *linear* convergence rate. Interestingly, our analysis establishes a link between f_{LS} in reparametrized coordinates (Eq. (7)) and the well-studied task of minimizing (generalized) Rayleigh quotients as it is commonly encountered in eigenvalue problems.

Convergence analysis To simplify the analysis, note that, for a given \mathbf{w} , the objective of Eq. (7) is convex w.r.t. the scalar g and thus the optimal value $g_{\mathbf{w}}^*$ can be found by setting $\frac{\partial f_{\text{LS}}}{\partial g} := 0$, which yields $g_{\mathbf{w}}^* := -(\mathbf{u}^\top \mathbf{w}) / \|\mathbf{w}\|_{\mathbf{S}}$. Replacing this closed-form solution into Eq. (7) yields the following optimization problem

$$\min_{\mathbf{w} \in \mathbb{R}^d} \left(\rho(\mathbf{w}) := -\frac{\mathbf{w}^\top \mathbf{u} \mathbf{u}^\top \mathbf{w}}{\mathbf{w}^\top \mathbf{S} \mathbf{w}} \right), \quad (8)$$

which, as discussed in Appendix A.2, is a special case of minimizing the generalized Rayleigh quotient for which an extensive literature exists [16, 9]. Here, we particularly consider solving (8) using Gradient Descent, which applies the following iterate updates to the parameters,

$$\mathbf{w}_{t+1} := \mathbf{w}_t + 2\eta_t \left((\mathbf{u}^\top \mathbf{w}_t) \mathbf{u} + \rho(\mathbf{w}_t) \mathbf{S} \mathbf{w}_t \right) / (\mathbf{w}_t^\top \mathbf{S} \mathbf{w}_t). \quad (9)$$

Based upon existing results, the next theorem establishes a convergence rate for the above iterates to the minimizer \mathbf{w}^* in the normalized coordinates.

Theorem 1. [Convergence rate on least squares] Suppose that the (weak) Assumption 1 on the data distribution holds. Consider the GD iterates $\{\mathbf{w}_t\}_{t \in \mathbb{N}^+}$ given in Eq. (9) with the stepsize $\eta_t = \mathbf{w}_t^\top \mathbf{S} \mathbf{w}_t / (2L|\rho(\mathbf{w}_t)|)$ and starting from $\rho(\mathbf{w}_0) \neq 0$. Then,

$$\rho(\mathbf{w}_t) - \rho(\mathbf{w}^*) \leq \left(1 - \frac{\mu}{L}\right)^{2t} (\rho(\mathbf{w}_0) - \rho(\mathbf{w}^*)). \quad (10)$$

Hence, $\rho(\mathbf{w}_t)$ linearly converges to $\rho(\mathbf{w}^*)$. Furthermore, the \mathbf{S}^{-1} -norm of the gradient $\nabla \rho(\mathbf{w}_t)$ relates to the suboptimality as

$$\|\mathbf{w}_t\|_{\mathbf{S}}^2 \|\nabla \rho(\mathbf{w}_t)\|_{\mathbf{S}^{-1}}^2 / 4\rho(\mathbf{w}_t) = \rho(\mathbf{w}_t) - \rho(\mathbf{w}^*). \quad (11)$$

Note that this convergence rate is similar to the rate of standard GD on the original objective f_{LS} (as presented in Eq. (6)) [24]. Yet, it is interesting to see that the non-convexity of the normalized objective does not slow gradient-based optimization down. In the upcoming sections, we will repeatedly invoke this result to analyze more complex objective functions for which GD – in the original coordinate space – only achieves a *sublinear* convergence rate.

4 Learning halfspaces

We now turn our attention to the problem of learning halfspaces, which encompasses training the simplest possible neural network, the Perceptron. This optimization problem can be written as

$$\min_{\tilde{\mathbf{w}} \in \mathbb{R}^d} \left(f_{\text{LH}}(\tilde{\mathbf{w}}) := \mathbf{E}_{y, \mathbf{x}} \left[\varphi(-y \mathbf{x}^\top \tilde{\mathbf{w}}) \right] = \mathbf{E}_{\mathbf{z}} \left[\varphi(\mathbf{z}^\top \tilde{\mathbf{w}}) \right] \right), \quad (12)$$

where $\varphi : \mathbb{R} \rightarrow \mathbb{R}^+$ is a loss function. Common choices for φ include the zero-one, piece-wise linear, logistic and sigmoidal loss. We here tailor our analysis to the following choice of loss function.

Assumption 3. [Assumptions on loss function] We assume that the loss function $\varphi : \mathbb{R} \rightarrow \mathbb{R}$ is infinitely differentiable, i.e. $\varphi \in C^\infty(\mathbb{R}, \mathbb{R})$, with a bounded derivative, i.e. $\exists \Phi > 0$ such that $|\varphi^{(1)}(\beta)| \leq \Phi, \forall \beta \in \mathbb{R}$.

We furthermore need f_{LH} to be sufficiently smooth, as presented in the next assumption.

Assumption 4. [Smoothness assumption] We assume that the objective $f : \mathbb{R}^d \rightarrow \mathbb{R}$ is ζ -smooth if it is differentiable on \mathbb{R} and its gradient is ζ -Lipschitz. Furthermore, we assume that a solution $\alpha^* := \arg \min_{\alpha} \|\nabla f(\alpha \mathbf{w})\|^2$ exists that is bounded in the sense that $\forall \mathbf{w} \in \mathbb{R}^d, -\infty < \alpha^* < \infty$.²

Since globally optimizing (12) is in general NP-hard [12], we instead focus on understanding the effect of the normalized parameterization when searching for a stationary point. We assume that \mathbf{z} is a multivariate normal random variable (Assumption 2). The use of simple inputs is rather common when analyzing complex systems, as is for example the case in signal processing where linear time-invariant systems are characterized by their impulse response [25]. Normality is also a

²This is a rather technical but not so restrictive assumption. For example for the sigmoid loss it always holds unless the classification error of \mathbf{w} is already zero.

common assumption in the analysis of neural networks, e.g. [5] showed that for a special type of one-hidden layer network with isotropic Gaussian inputs, all local minimizers are global. Under the same assumption, similar results for different classes of neural networks were derived in [21, 29, 8].

4.1 Global characterization of the objective

The learning halfspaces objective f_{LH} – on Gaussian inputs – has a remarkable property: all critical points lie on the same line, independent of the choice of the loss function φ . We formalize this claim in the next lemma.

Lemma 1. *Under Assumptions 1 and 2, all bounded critical points $\tilde{\mathbf{w}}_*$ of f_{LH} have the general form*

$$\tilde{\mathbf{w}}_* = g_* \mathbf{S}^{-1} \mathbf{u},$$

where the scalar $g_* \in \mathbb{R}$ depends on $\tilde{\mathbf{w}}_*$ and the choice of the loss function φ .

Interestingly, the optimal direction of these critical points spans the same line as the solution of ordinary least-squares regression (compare Eq. (30)). This fact was first pointed out in [4] in the context of convex optimization of generalized linear models. Exploiting this property, [10] proposed a two-step global optimization procedure for generalized linear models, which first involves finding the optimal direction by optimizing least-squares as a surrogate objective and secondly searching for a proper scaling factor (in one dimension). However, classical optimization methods which perform updates based on local information are generally blind to such global properties of the objective. Yet, running a local optimization method in coordinates reparameterized as in (4) allows these methods to exploit the above property by splitting the optimization problem into searching for the optimal direction and optimal scaling separately. Based upon this observation we will show that GD achieves a provably faster rate in the normalized space than in original coordinates.

4.2 Local optimization in normalized parameterization

Let $f_{\text{LH}}(\mathbf{w}, g)$ be the \mathbf{S} -reparameterized objective with $\tilde{\mathbf{w}} = g\mathbf{w}/\|\mathbf{w}\|_{\mathbf{S}}$ as defined in Eq. (4). We here consider optimizing this objective using a variant of GD in normalized parameter space named GDNP (Algorithm 1). In each iteration, GDNP first performs a gradient step to optimize f_{LH} with respect to the direction \mathbf{w} and then does a one-dimensional bisection search to estimate the scaling factor g . It is therefore a slight modification of the usual GD in normalized parameterization (i.e. BN): instead of one gradient step on the scalar g , we search for the (locally)-optimal g at each iteration. This modification simplifies the theoretical analysis but can easily be substituted in practice by performing multiple GD steps on the scaling factor.

4.3 Convergence result

We analyze the convergence of Algorithm 1 on f_{LH} with Gaussian inputs. The next theorem establishes a linear convergence rate to a critical point. Note that the stepsize s_t can be computed efficiently.

Algorithm 1 Gradient Descent in Normalized Parameterization (GDNP)

```

1: Input:  $T_d, T_s$ , stepsize policy  $s$ , stopping criterion  $h$  and objective  $f$ 
2:  $g \leftarrow 1$ , and initialize  $\mathbf{w}_0$  such that  $\rho(\mathbf{w}_0) \neq 0$ 
3: for  $t = 1, \dots, T_d$  do
4:   if  $h(\mathbf{w}_t, g_t) \neq 0$  then
5:      $s_t \leftarrow s(\mathbf{w}_t, g_t)$ 
6:      $\mathbf{w}_{t+1} \leftarrow \mathbf{w}_t - s_t \nabla_{\mathbf{w}} f(\mathbf{w}_t, g_t)$            # directional step
7:   end if
8:   Choose  $a_t^{(0)}$  and  $b_t^{(0)}$  such that  $\partial_g f(a_t^{(0)}, \mathbf{w}_t) \cdot \partial_g f(b_t^{(0)}, \mathbf{w}_t) > 0$ .
9:    $g_t \leftarrow \text{Bisection}(T_s, a_t^{(0)}, b_t^{(0)}, f)$            # scaling step (see Alg. 3)
10: end for
11:  $\tilde{\mathbf{w}}_{T_d} \leftarrow g_{T_d} \mathbf{w}_{T_d} / \|\mathbf{w}_{T_d}\|_{\mathbf{s}}$ 
12: return  $\tilde{\mathbf{w}}_{T_d}$ 

```

Theorem 2. [Convergence rate of GDNP on learning halfspaces] Suppose Assumptions 1–4 hold. Let $\tilde{\mathbf{w}}_{T_d}$ be the output of GDNP on f_{LH} with the following choice of stepsizes

$$s_t := s(\mathbf{w}_t, g_t) = -\|\mathbf{w}_t\|_{\mathbf{S}}^3 / \left(L g_t h(\mathbf{w}_t, g_t) \mathbf{u}^\top \mathbf{w}_t \right), \quad t = 1, \dots, T_d, \quad (13)$$

where $h(\mathbf{w}_t, g_t) = \mathbf{E}_{\mathbf{z}} [\varphi'(g_t \mathbf{z}^\top \mathbf{w}_t / \|\mathbf{w}_t\|_{\mathbf{s}})] \neq 0$ is a stopping criterion. If $\rho(\mathbf{w}_0) \neq 0$ (see Eq. (8)), then $\tilde{\mathbf{w}}_{T_d}$ is an approximate critical point of f_{LH} in the sense that

$$\|\nabla_{\tilde{\mathbf{w}}} f(\tilde{\mathbf{w}}_{T_d})\|^2 \leq (1 - \mu/L)^{2T_d} \Phi^2 (\rho(\mathbf{w}_0) - \rho^*) + 2^{-T_s} \zeta |b_t^{(0)} - a_t^{(0)}| / \mu^2. \quad (14)$$

4.4 Advantage of S-normalization

We compare the computational cost of GD, Nesterov’s accelerated gradient descent (AGD) and GDNP to reach an ϵ -optimality critical point $\tilde{\mathbf{w}}$ (i.e. a point $\tilde{\mathbf{w}}$ such that $\|\nabla_{\tilde{\mathbf{w}}} f_{\text{LH}}(\tilde{\mathbf{w}})\| \leq \epsilon$). The results are presented in Table 1, where $\mathcal{O}(T_{\text{gd}})$ represents the time complexity of computing a gradient for each method (either in the original or the normalized parametrization). Although we observe that the accelerated rate achieved by GDNP is significantly better than the best known rate of AGD for non-convex objective functions, we need to point out that the rate for GDNP relies on the Gaussian assumption of the data distribution. Yet, Section 4.5 includes promising experimental results in a more practical setting with non-Gaussian data.

Method	Assumptions	Complexity	Rate	Reference
GD	Smoothness	$\mathcal{O}(T_{\text{gd}} \epsilon^{-2})$	Sublinear	[24]
AGD	Smoothness	$\mathcal{O}(T_{\text{gd}} \epsilon^{-7/4} \log(1/\epsilon))$	Sublinear	[6]
AGD	Smoothness+convexity	$\mathcal{O}(T_{\text{gd}} \epsilon^{-1})$	Sublinear	[24]
GDNP	1, 2, 3, and 4	$\mathcal{O}(T_{\text{gd}} \log^2(1/\epsilon))$	Linear	This paper

Table 1: Computational complexity to reach an ϵ -critical point on f_{LH} – with a (possibly) non-convex loss function φ . Note that GD and AGD also achieve a linear convergence rate under a rather strong assumption on f_{LS} , i.e. strong convexity

4.5 Experiments I

In order to substantiate the above analysis we compare the convergence behavior of GD and AGD to three versions of Gradient Descent in normalized coordinates. Namely, we assess (i) GDNP as stated in Algorithm 1, (ii) a simpler version (BN) which simultaneously updates \mathbf{w} and \mathbf{g} with one GD step on each parameter³ and (iii) Weight Normalization (WN) as presented in [27]. All methods use full batch sizes.

We consider empirical risk minimization as a surrogate for (12) on the common realworld dataset *a9a* as well as on synthetic data drawn from a multivariate gaussian distribution. We center the datasets and use two different functions $\varphi(\cdot)$. First, we choose the *softplus* which resembles the classical logistic regression (convex). Secondly, we use the *sigmoid* which is a commonly used (non-convex) continuous approximation of the 0-1 loss [31]. Except for GDNP, each method is run with a problem specific, constant stepsize which is grid-searched in the first- and chosen as the inverse of the gradient Lipschitz constant in the second setting. Further details can be found in Appendix D.

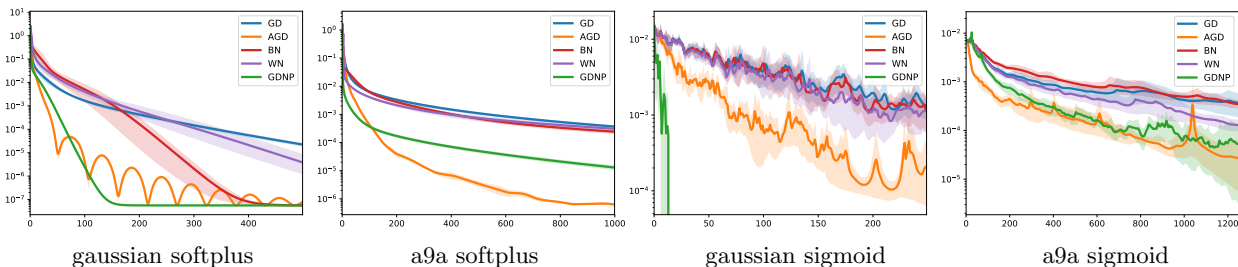


Figure 1: Results of an average run (solid line) in terms of log suboptimality (softplus) and log gradient norm (sigmoid) over iterations as well as 90% confidence intervals of 10 runs with random initialization.

The Gaussian design experiments clearly confirm Theorem 4 in the sense that the loss in the convex-, as well as the gradient norm in the non-convex case decrease at a linear rate. The results on *a9a* show that GDNP can accelerate optimization even when the normality assumption does not hold and in a setting where no covariate shift is present, which motivates future research of normalization techniques in optimization. Interestingly, the performance of simple BN and WN is similar to that of GD, which suggests that the length-direction decoupling on its own does not capture the entire potential of these methods. On the other hand, GDNP takes full advantage of the parameter splitting, both in terms of bisection in scalar g and adaptive stepsizes in \mathbf{w} . It is an exciting open question whether similar techniques somewhere in between the two extremes can be developed to speed up the training of Neural Networks.

5 Neural networks

We now turn our focus to optimizing the weights of a multilayer perceptron (MLP) with one hidden layer and m hidden units that maps an input $\mathbf{x} \in \mathbb{R}^d$ to a scalar output in the following way

$$F(\mathbf{x}, \tilde{\mathbf{W}}, \Theta) = \sum_{i=1}^m \theta_i \varphi(\mathbf{x}^\top \tilde{\mathbf{w}}^{(i)}), \quad \tilde{\mathbf{W}} := \{\tilde{\mathbf{w}}^{(1)}, \dots, \tilde{\mathbf{w}}^{(m)}\}, \quad \Theta := \{\theta^{(1)}, \dots, \theta^{(m)}\}.$$

³Thus BN is conceptually very close to the classical Batch Normalization presented in [14]

The $\tilde{\mathbf{w}}^{(i)} \in \mathbb{R}^d$ and $\theta^{(i)} \in \mathbb{R}$ terms are the input and output weights of unit i and $\varphi : \mathbb{R} \rightarrow \mathbb{R}$ is a so-called activation function. We assume φ to be a tanh, which is a common choice in many neural network architectures used in practice. Given a loss function $\ell : \mathbb{R} \rightarrow \mathbb{R}^+$, the optimal input- and output weights are determined by minimizing the following optimization problem

$$\min_{\tilde{\mathbf{W}}, \Theta} \left(f_{\text{NN}}(\tilde{\mathbf{W}}, \Theta) := \mathbf{E}_{y, \mathbf{x}} \left[\ell \left(-yF(\mathbf{x}, \tilde{\mathbf{W}}, \Theta) \right) \right] \right) \quad (15)$$

In the following, we analyze optimization of the input weights $\tilde{\mathbf{W}}$ with frozen output weights Θ and thus write $F(\tilde{\mathbf{W}})$ hereafter for simplicity. As previously assumed for the case of learning halfspaces, our analysis relies on the normality assumption under which f_{NN} exhibits a similar global characterization to the objective of learning halfspaces⁴. Clearly, the normality assumption does not necessarily hold on real datasets. However, we will see that it still yields useful insights which can be extended to more realistic settings, as the experimental results in Section 5.3 suggest.

5.1 Optimization in normalized parameterization

We again consider normalizing the weights of each unit by means of its input covariance matrix \mathbf{S} , i.e. $\tilde{\mathbf{w}}^{(i)} = g^{(i)} \mathbf{w}^{(i)} / \|\mathbf{w}^{(i)}\|_{\mathbf{S}}$, $\forall i = 1, \dots, m$. In the following we present a simple way to leverage the input-output decoupling in an algorithmic manner. Contrary to BN, which optimizes all the weights simultaneously, our approach is based on alternating optimization over the different hidden units. We introduce this modification to simplify the theoretical analysis.

Algorithm 2 Training an MLP with GDNP

- 1: Input: $T_d^{(i)}, T_s^{(i)}$, step-size policies $s^{(i)}$, stopping criterion $h^{(i)}$
 - 2: $\mathbf{W}_{/1} \leftarrow \mathbf{0}, \mathbf{g}_{/1} = \mathbf{1}$
 - 3: **for** $i = 1, \dots, m$ **do**
 - 4: $\mathbf{W}_{/i} := \{\mathbf{w}^{(1)}, \dots, \mathbf{w}^{(i-1)}, \mathbf{w}^{(i+1)}, \dots, \mathbf{w}^{(m)}\}, \mathbf{g}_{/i} := \{g^{(1)}, \dots, g^{(i-1)}, g^{(i+1)}, \dots, g^{(m)}\}$
 - 5: $f^{(i)}(\mathbf{w}^{(i)}, g^{(i)}) := f_{\text{NN}}(\mathbf{w}^{(i)}, g^{(i)}, \mathbf{W}_{/i}, \mathbf{g}_{/i})$
 - 6: $(\mathbf{w}^{(i)}, g^{(i)}) \leftarrow \text{GDNP}(f^{(i)}, T_d^{(i)}, T_s^{(i)}, s^{(i)}, h^{(i)})$ # optimization of unit i
 - 7: **end for**
 - 8: **return** $\mathbf{W} := [\mathbf{w}^{(1)}, \dots, \mathbf{w}^{(m)}], \mathbf{g} := [g^1, \dots, g^m]$.
-

5.2 Convergence result

We adapt GDNP to the problem of optimizing the units of a neural network (Algorithm 2). As mentioned above, we analyze an approach where we optimize each unit independently which formally results in optimizing the function $f^{(i)}(\mathbf{w}^{(i)}, g^{(i)})$ which is more explicitly defined in Algorithm 2. In the next theorem, we prove that GDNP achieves a linear rate of convergence to optimize each $f^{(i)}$.

Theorem 3. *[Convergence of GDNP on MLP] Suppose Assumptions 1–4 hold. We consider optimizing the weights $(\mathbf{w}^{(i)}, g^{(i)})$ of unit i , assuming that all directions $\{\mathbf{w}^{(j)}\}_{j < i}$ are critical points of f_{NN}*

⁴The learning halfspace result is discussed in Section 4.1. See Appendix C for further details on the neural network extension.

and $\mathbf{w}^k = \mathbf{0}$ for $k > i$. Then, GDNP with step-size policy $s^{(i)}$ as in (85) and stopping criterion $h^{(i)}$ as in (86) yields a linear convergence rate on $f^{(i)}$ in the sense that

$$\|\nabla_{\tilde{\mathbf{w}}^{(i)}} f(\tilde{\mathbf{w}}_t^{(i)})\|_{\mathbf{S}^{-1}}^2 \leq (1 - \mu/L)^{2t} C (\rho(\mathbf{w}_0) - \rho^*) + 2^{-T_s^{(i)}} \zeta |b_t^{(0)} - a_t^{(0)}|/\mu^2, \quad (16)$$

where the constant $C > 0$ is defined in Eq. (89).

The result of Theorem 3 relies on the fact that each $\mathbf{w}^{(j)}$, $j \neq i$ is either zero or fully optimized. We believe that the result holds for approximately optimal weights, but the analysis of this case is more involved. To complete the picture, we prove that Algorithm 2 guarantees the optimality condition to be fulfilled asymptotically.

Lemma 2. Consider $\mathbf{W}_{/i} := \{\mathbf{w}^{(j)}\}_{j < i} \cup \{\mathbf{w}^{(k)} = \mathbf{0}\}_{k > i}$ in Algorithm 2. Then $\mathbf{w}^{(j)}$ are critical points of f_{NN} for $j < i$ and $(T_d^{(j)}, T_s^{(j)}) \rightarrow (\infty, \infty)$.

Since the convergence of Algorithm 2 is in practice fast on each unit, we hypothesize that the optimum is reached within a finite number of iterations.

5.3 Experiments II

In the proof of Theorem 3 we show that GDNP can leverage the length-direction decoupling in a way that lowers cross-dependencies between hidden layers and yields faster convergence. A central part of the proof is a generalization of Lemma 1 to Neural Networks which says that, given Gaussian inputs, the optimal direction of a given layer is independent of all downstream layers (Appendix C). Since this assumption is rather strong and since Algorithm 2 is intended for analysis purposes only, we test the validity of the above hypothesis outside the Gaussian setting by training a feedforward network on the an image classification task with the far simpler BN method presented in Section 4.5. For comparison, a second network is trained by standard GD and we measure the cross-dependencies of layers in terms of the Frobenius norm of the second partial cross derivatives.

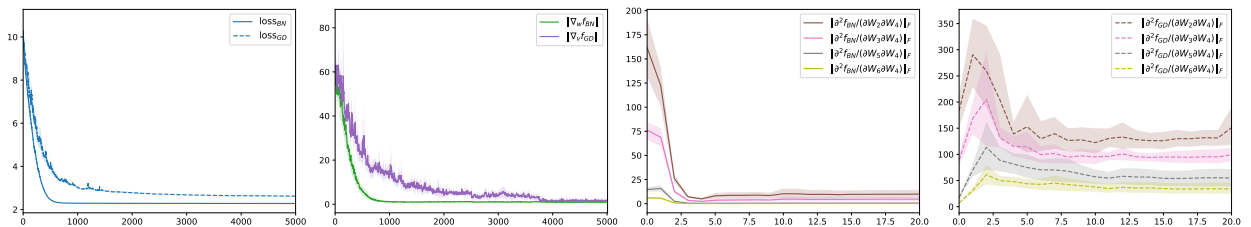


Figure 2: (i) Loss, (ii) gradient norm and dependencies between central- and all other layers for BN (iii) and GD (iv) on a 6 hidden layer network with 50 units (each) on the CIFAR10 dataset (5 runs with random initialization).

Figure 2 confirms that the directional gradients of the central layer are indeed affected far more by the upstream than by the downstream layers and interestingly this holds even before reaching a critical point. The cross-dependencies are generally decaying for BN while they remain elevated in the GD network, which suggest that BN is indeed able to exploit the length-direction decoupling

to simplify the networks curvature structure and gradient trajectories for faster convergence. Of course, we cannot fully untangle this effect from the covariate shift reduction that was mentioned in the introduction. Yet, the fact that the decoupling increases in the distance to the middle layer emphasizes the relevance of further analysis particularly for deep neural network structures.

6 Conclusion

We took a theoretical approach to study the acceleration provided by Batch Normalization. Under a somewhat simplified setting, we have shown that the reparametrization performed by Batch Normalization leads to a provable acceleration of gradient-based optimization by splitting it into subtasks that are easier to solve. Note that our analysis does not consider covariate shift, it is therefore still an open question as to whether this aspect can lead to similar results. In order to evaluate the impact of the assumptions required for our analysis, we also performed experiments on real-world datasets that agree with the results of the theoretical analysis to a surprisingly large extent.

We consider this work as a first step for two particular directions of future research. First, it raises the question of how to optimally train Neural Networks with Batch Normalization. Particularly, the results of Section 5 suggest that different and adaptive stepsize schemes for the two parameters - length and direction - can lead to significant accelerations. Second, the analysis of Section 3 and 4 reveals that a better understanding of non-linear coordinate transformations is a promising direction for the continuous optimization community.

References

- [1] P-A Absil, Robert Mahony, and Rodolphe Sepulchre. *Optimization algorithms on matrix manifolds*. Princeton University Press, 2009.
- [2] Devansh Arpit, Yingbo Zhou, Bhargava U Kota, and Venu Govindaraju. Normalization propagation: A parametric technique for removing internal covariate shift in deep networks. *arXiv preprint arXiv:1603.01431*, 2016.
- [3] Jimmy Lei Ba, Jamie Ryan Kiros, and Geoffrey E Hinton. Layer normalization. *arXiv preprint arXiv:1607.06450*, 2016.
- [4] David R Brillinger. A generalized linear model with gaussian regressor variables. In *Selected Works of David Brillinger*, pages 589–606. Springer, 2012.
- [5] Alon Brutzkus and Amir Globerson. Globally optimal gradient descent for a convnet with gaussian inputs. *arXiv preprint arXiv:1702.07966*, 2017.
- [6] Yair Carmon, John C Duchi, Oliver Hinder, and Aaron Sidford. Accelerated methods for non-convex optimization. *arXiv preprint arXiv:1611.00756*, 2016.
- [7] Minhyung Cho and Jaehyung Lee. Riemannian approach to batch normalization. In I. Guyon, U. V. Luxburg, S. Bengio, H. Wallach, R. Fergus, S. Vishwanathan, and R. Garnett, editors, *Advances in Neural Information Processing Systems 30*, pages 5225–5235. Curran Associates, Inc., 2017.
- [8] Simon S Du, Jason D Lee, Yuandong Tian, Barnabas Poczos, and Aarti Singh. Gradient descent learns one-hidden-layer cnn: Don’t be afraid of spurious local minima. *arXiv preprint arXiv:1712.00779*, 2017.
- [9] Eugene G D’yakonov and Steve McCormick. *Optimization in solving elliptic problems*. CRC Press, 1995.

- [10] Murat A Erdogdu, Lee H Dicker, and Mohsen Bayati. Scaled least squares estimator for glms in large-scale problems. In *Advances in Neural Information Processing Systems*, pages 3324–3332, 2016.
- [11] Igor Gitman and Boris Ginsburg. Comparison of batch normalization and weight normalization algorithms for the large-scale image classification. *arXiv preprint arXiv:1709.08145*, 2017.
- [12] Venkatesan Guruswami and Prasad Raghavendra. Hardness of learning halfspaces with noise. *SIAM Journal on Computing*, 39(2):742–765, 2009.
- [13] Kaiming He, Xiangyu Zhang, Shaoqing Ren, and Jian Sun. Deep residual learning for image recognition. In *Proceedings of the IEEE conference on computer vision and pattern recognition*, pages 770–778, 2016.
- [14] Sergey Ioffe and Christian Szegedy. Batch normalization: Accelerating deep network training by reducing internal covariate shift. In *Proceedings of the 32Nd International Conference on International Conference on Machine Learning - Volume 37, ICML’15*, pages 448–456. JMLR.org, 2015.
- [15] Günter Klambauer, Thomas Unterthiner, Andreas Mayr, and Sepp Hochreiter. Self-normalizing neural networks. In *Advances in Neural Information Processing Systems*, pages 972–981, 2017.
- [16] Andrew V Knyazev. Preconditioned eigensolvers an oxymoron. *Electron. Trans. Numer. Anal.*, 7:104–123, 1998.
- [17] Andrew V Knyazev and Klaus Neymeyr. A geometric theory for preconditioned inverse iteration iii: A short and sharp convergence estimate for generalized eigenvalue problems. *Linear Algebra and its Applications*, 358(1-3):95–114, 2003.
- [18] AV Knyazev and AL Shorokhodov. On exact estimates of the convergence rate of the steepest ascent method in the symmetric eigenvalue problem. *Linear algebra and its applications*, 154:245–257, 1991.
- [19] Alex Krizhevsky and Geoffrey Hinton. Learning multiple layers of features from tiny images. 2009.
- [20] Zinoviy Landsman and Johanna Nevslehová. Stein’s lemma for elliptical random vectors. *Journal of Multivariate Analysis*, 99(5):912–927, 2008.
- [21] Yuanzhi Li and Yang Yuan. Convergence analysis of two-layer neural networks with relu activation. In *Advances in Neural Information Processing Systems*, pages 597–607, 2017.
- [22] James Martens, Ilya Sutskever, and Kevin Swersky. Estimating the hessian by back-propagating curvature. *arXiv preprint arXiv:1206.6464*, 2012.
- [23] VS Mikhalevich, NN Redkovskii, and AA Antonyuk. Minimization methods for smooth nonconvex functions. *Cybernetics*, 24(4):395–403, 1988.
- [24] Yurii Nesterov. *Introductory lectures on convex optimization: A basic course*, volume 87. Springer Science & Business Media, 2013.
- [25] Alan V Oppenheim. *Discrete-time signal processing*. Pearson Education India, 1999.
- [26] Adam Paszke, Sam Gross, Soumith Chintala, Gregory Chanan, Edward Yang, Zachary DeVito, Zeming Lin, Alban Desmaison, Luca Antiga, and Adam Lerer. Automatic differentiation in pytorch. In *NIPS-W*, 2017.
- [27] Tim Salimans and Diederik P Kingma. Weight normalization: A simple reparameterization to accelerate training of deep neural networks. In *Advances in Neural Information Processing Systems*, pages 901–909, 2016.
- [28] Shibani Santurkar, Dimitris Tsipras, Andrew Ilyas, and Aleksander Madry. How does batch normalization help optimization?(no, it is not about internal covariate shift). *arXiv preprint arXiv:1805.11604*, 2018.
- [29] Mahdi Soltanolkotabi, Adel Javanmard, and Jason D Lee. Theoretical insights into the optimization landscape of over-parameterized shallow neural networks. *arXiv preprint arXiv:1707.04926*, 2017.

- [30] Christian Szegedy, Sergey Ioffe, Vincent Vanhoucke, and Alexander A Alemi. Inception-v4, inception-resnet and the impact of residual connections on learning. In *AAAI*, volume 4, page 12, 2017.
- [31] Yuchen Zhang, Jason D Lee, Martin J Wainwright, and Michael I Jordan. Learning halfspaces and neural networks with random initialization. *arXiv preprint arXiv:1511.07948*, 2015.

Appendix

A Analysis of Least-squares

A.1 Restated result

Recall that, after normalizing according to (4) and using the closed form solution for the optimal scaling factor $g^* := -(\mathbf{u}^\top \mathbf{w}) / \|\mathbf{w}\|_{\mathbf{S}}$, optimizing the ordinary least squares objective can be written as the following minimization problem

$$\min_{\mathbf{w} \in \mathbb{R}^d} \left(\rho(\mathbf{w}) := -\frac{\mathbf{w}^\top \mathbf{u} \mathbf{u}^\top \mathbf{w}}{\mathbf{w}^\top \mathbf{S} \mathbf{w}} \right). \quad (8 \text{ revisited})$$

We consider optimizing the above objective by GD which takes iterative steps of the form

$$\mathbf{w}_{t+1} = \mathbf{w}_t - \eta_t \nabla \rho(\mathbf{w}_t), \quad (17)$$

where

$$\nabla \rho(\mathbf{w}_t) = -2(\mathbf{B} \mathbf{w}_t + \rho(\mathbf{w}_t) \mathbf{S} \mathbf{w}_t) / \mathbf{w}_t^\top \mathbf{S} \mathbf{w}_t. \quad (18)$$

Furthermore, we choose

$$\eta_t = \frac{\mathbf{w}_t^\top \mathbf{S} \mathbf{w}_t}{2L|\rho(\mathbf{w}_t)|}. \quad (19)$$

Assumption 1. [Weak assumption on data distribution] We assume that $\mathbf{E}[\mathbf{x}] = \mathbf{0}$. We further assume that the spectrum of the matrix \mathbf{S} is bounded as

$$0 < \mu := \lambda_{\min}(\mathbf{S}), L := \lambda_{\max}(\mathbf{S}) < \infty. \quad (2)$$

As a result, \mathbf{S} is the symmetric positive definite covariance matrix of \mathbf{x} .

It is noteworthy that $\rho(\mathbf{w}) \leq 0, \forall \mathbf{w} \in \mathbb{R}^d \setminus \{\mathbf{0}\}$ under the above assumption. In the next theorem, we establish a convergence rate of GD in terms of function value as well as gradient norm.

Theorem 1. [Convergence rate on least squares] Suppose that the (weak) Assumption 1 on the data distribution holds. Consider the GD iterates $\{\mathbf{w}_t\}_{t \in \mathbb{N}^+}$ given in Eq. (9) with the stepsize $\eta_t = \mathbf{w}_t^\top \mathbf{S} \mathbf{w}_t / (2L|\rho(\mathbf{w}_t)|)$ and starting from $\rho(\mathbf{w}_0) \neq 0$. Then,

$$\rho(\mathbf{w}_t) - \rho(\mathbf{w}^*) \leq \left(1 - \frac{\mu}{L}\right)^{2t} (\rho(\mathbf{w}_0) - \rho(\mathbf{w}^*)). \quad (10)$$

Hence, $\rho(\mathbf{w}_t)$ linearly converges to $\rho(\mathbf{w}^*)$. Furthermore, the \mathbf{S}^{-1} -norm of the gradient $\nabla \rho(\mathbf{w}_t)$ relates to the suboptimality as

$$\|\mathbf{w}_t\|_{\mathbf{S}}^2 \|\nabla \rho(\mathbf{w}_t)\|_{\mathbf{S}^{-1}}^2 / 4|\rho(\mathbf{w}_t)| = \rho(\mathbf{w}_t) - \rho(\mathbf{w}^*). \quad (11)$$

The proof of this result crucially relies on the insight that the minimization problem given in (7) resembles the problem of maximizing the generalized Rayleigh quotient which is commonly encountered in generalized eigenproblems. We will thus first review this area, where convergence rates are usually provided in terms of the angle of the current iterate with the maximizer, which is the principal eigenvector. Interestingly, this angle can be related to both, the current function value as well as the the norm of the current gradient. We will make use of these connections to prove the above Theorem in Section A.5. Although not necessarily needed for convex function, we introduce the gradient norm relation as we will later go on to prove a similar result for possibly non-convex functions in the learning halfspace setting (Theorem 4).

A.2 Background on eigenvalue problems

A.2.1 Rayleigh quotient

Optimizing the Rayleigh quotient is a classical non-convex optimization problem that is often encountered in eigenvector problems. Let $\mathbf{B} \in \mathbb{R}^{d \times d}$ be a symmetric matrix, then $\mathbf{w}^1 \in \mathbb{R}^d$ is the principal eigenvector of \mathbf{B} if it maximizes

$$q(\mathbf{w}) = \frac{\mathbf{w}^\top \mathbf{B} \mathbf{w}}{\mathbf{w}^\top \mathbf{w}} \quad (20)$$

and $q(\mathbf{w})$ is called the Rayleigh quotient. Notably, this quotient satisfies the so-called Rayleigh inequality

$$\lambda_{\min}(\mathbf{B}) \leq q(\mathbf{w}) \leq \lambda_1(\mathbf{B}), \quad \forall \mathbf{w} \in \mathbb{R} \setminus \{\mathbf{0}\},$$

where $\lambda_{\min}(\mathbf{B})$ and $\lambda_1(\mathbf{B})$ are the smallest and largest eigenvalue of \mathbf{B} respectively.

Maximizing $q(\mathbf{w})$ is a non-convex (strict-saddle) optimization problem, where the i -th critical point \mathbf{v}_i constitutes the i -th eigenvector with corresponding eigenvalue $\lambda_i = q(\mathbf{w}_i)$ (see [1], Section 4.6.2 for details). It is known that optimizing $q(\mathbf{w})$ with GD - using an iteration-dependent stepsize - converges linearly to the principal eigenvector \mathbf{v}_1 . The convergence analysis is based on the "minidimensional" method and yields the following result

$$\frac{\lambda_1 - q(\mathbf{w}_t)}{\cos^2 \angle(\mathbf{w}_t, \mathbf{v}_1)} \leq \left(1 - \frac{\lambda_1 - \lambda_2}{\lambda_1 - \lambda_{\min}}\right)^{2t} \frac{\lambda_1 - q(\mathbf{w}_0)}{\cos^2 \angle(\mathbf{w}_0, \mathbf{v}_1)} \quad (21)$$

under weak assumptions on \mathbf{w}_0 . Details as well as the proof of this result can be found in [18].

A.2.2 Generalized rayleigh quotient

The reparametrized least squares objective (8), however, is not exactly equivalent to (20) because of the covariance matrix that appears in the denominator. As a matter of fact, our objective is a special instance of the generalized Rayleigh quotient

$$\tilde{\rho}(\mathbf{w}) = \frac{\mathbf{w}^\top \mathbf{B} \mathbf{w}}{\mathbf{w}^\top \mathbf{A} \mathbf{w}}, \quad (22)$$

where \mathbf{B} is defined as above and $\mathbf{A} \in \mathbb{R}^{d \times d}$ is a symmetric positive definite matrix.

Maximizing (22) is a generalized eigenproblem in the sense that it solves the task of finding eigenvalues λ of the matrix pencil (\mathbf{B}, \mathbf{A}) for which $\det(\mathbf{B} - \lambda \mathbf{A}) = 0$, i.e. finding a vector \mathbf{v} that obeys $\mathbf{B} \mathbf{v} = \lambda \mathbf{A} \mathbf{v}$. Again we have

$$\lambda_{\min}(\mathbf{B}, \mathbf{A}) \leq \tilde{\rho}(\mathbf{w}) \leq \lambda_1(\mathbf{B}, \mathbf{A}), \quad \forall \mathbf{w} \in \mathbb{R} \setminus \{0\}.$$

Among the rich literature on solving generalized symmetric eigenproblems, a GD convergence rate similar to (21) has been established in Theorem 6 of [17], which yields

$$\frac{\lambda_1 - \rho(\mathbf{w}_{t+1})}{\rho(\mathbf{w}_{t+1}) - \lambda_2} \leq \left(1 - \frac{\lambda_1 - \lambda_2}{\lambda_1 - \lambda_{\min}}\right)^{2t} \frac{\lambda_1 - \rho(\mathbf{w}_t)}{\rho(\mathbf{w}_t) - \lambda_2},$$

again under weak assumptions on \mathbf{w}_0 .

A.2.3 Our contribution

Since our setting in Eq. (8) is a minimization task, we note that for our specific choice of \mathbf{A} and \mathbf{B} we have $-\tilde{\rho}(\mathbf{w}) = \rho(\mathbf{w})$ and we recall the general result that then

$$\min \rho(\mathbf{w}) = -\max(\tilde{\rho}(\mathbf{w})).$$

More importantly, we here have a special case where the nominator of $\rho(\mathbf{w})$ has a particular low rank structure. In fact, $\mathbf{B} := \mathbf{u} \mathbf{u}^\top$ is a rank one matrix. Instead of directly invoking the convergence rate in [17], this allows

for a much simpler analysis of the convergence rate of GD on $\rho(\mathbf{w})$ since the rank one property yields a simpler representation of the relevant vectors. Furthermore, we establish a connection between suboptimality on function value and the \mathbf{S}^{-1} -norm of the gradient. As mentioned earlier, we need such a guarantee in our future analysis on learning halfspaces which is an instance of a (possibly) non-convex optimization problem.

A.3 Preliminaries

Notations Let \mathbf{A} be a symmetric positive definite matrix. We introduce the following compact notations that will be used throughout the analysis.

- **A-inner product** of $\mathbf{w}, \mathbf{v} \in \mathbb{R}^d$: $\langle \mathbf{w}, \mathbf{v} \rangle_{\mathbf{A}} = \mathbf{w}^{\top} \mathbf{A} \mathbf{v}$.
- **A-norm** of $\mathbf{w} \in \mathbb{R}^d$: $\|\mathbf{w}\|_{\mathbf{A}} = (\mathbf{w}^{\top} \mathbf{A} \mathbf{w})^{1/2}$.
- **A-angle** between two vectors $\mathbf{w}, \mathbf{v} \in \mathbb{R}^d \setminus \{\mathbf{0}\}$:

$$\angle_{\mathbf{A}}(\mathbf{w}, \mathbf{v}) := \arccos\left(\frac{\langle \mathbf{w}, \mathbf{v} \rangle_{\mathbf{A}}}{\|\mathbf{w}\|_{\mathbf{A}} \|\mathbf{v}\|_{\mathbf{A}}}\right) \quad (23)$$

- **A-orthogonal projection** $\hat{\mathbf{w}}$ of \mathbf{w} to $\text{span}\{\mathbf{v}\}$ for $\mathbf{w}, \mathbf{v} \in \mathbb{R}^d \setminus \{\mathbf{0}\}$:

$$\hat{\mathbf{w}} \in \text{span}\{\mathbf{v}\} \quad \text{with} \quad \langle \mathbf{w} - \hat{\mathbf{w}}, \mathbf{v} \rangle_{\mathbf{A}} = 0 \quad (24)$$

- **A-spectral norm** of a matrix $\mathbf{C} \in \mathbb{R}^{d \times d}$:

$$\|\mathbf{C}\|_{\mathbf{A}} := \max_{\mathbf{w} \in \mathbb{R}^d \setminus \{\mathbf{0}\}} \frac{\|\mathbf{C}\mathbf{w}\|_{\mathbf{A}}}{\|\mathbf{w}\|_{\mathbf{A}}} \quad (25)$$

These notations allow us to make the analysis similar to the simple Rayleigh quotient case. For example, the denominator in (22) can now be written as $\|\mathbf{w}\|_{\mathbf{A}}^2$.

Properties We will use the following elementary properties of the induced terms defined above.

(P.1) $\sin^2 \angle_{\mathbf{A}}(\mathbf{w}, \mathbf{v}) = 1 - \cos^2 \angle_{\mathbf{A}}(\mathbf{w}, \mathbf{v})$

(P.2) If $\hat{\mathbf{w}}$ is the **A-orthogonal** projection of \mathbf{w} to $\text{span}\{\mathbf{v}\}$, then it holds that

$$\cos^2 \angle_{\mathbf{A}}(\mathbf{w}, \mathbf{v}) = \frac{\|\hat{\mathbf{w}}\|_{\mathbf{A}}^2}{\|\mathbf{w}\|_{\mathbf{A}}^2}, \quad \sin \angle_{\mathbf{A}} \mathbf{w} \mathbf{v} = \frac{\|\mathbf{w} - \hat{\mathbf{w}}\|_{\mathbf{A}}}{\|\mathbf{w}\|_{\mathbf{A}}} \quad (26)$$

(P.3) The **A-spectral** norm of a matrix can be written in the alternative form

$$\|\mathbf{C}\|_{\mathbf{A}} = \max_{\mathbf{w} \in \mathbb{R}^d \setminus \{\mathbf{0}\}} \frac{\|\mathbf{A}^{1/2} \mathbf{C} \mathbf{w}\|_2}{\|\mathbf{A}^{1/2} \mathbf{w}\|_2} = \max_{\mathbf{w} \in \mathbb{R}^d \setminus \{\mathbf{0}\}} \frac{\|(\mathbf{A}^{1/2} \mathbf{C} \mathbf{A}^{-1/2}) \mathbf{A}^{1/2} \mathbf{w}\|_2}{\|\mathbf{A}^{1/2} \mathbf{w}\|_2} \quad (27)$$

$$= \|\mathbf{A}^{1/2} \mathbf{C} \mathbf{A}^{-1/2}\|_2 \quad (28)$$

(P.4) Let $\mathbf{C} \in \mathbb{R}^{d \times d}$ be a square matrix and $\mathbf{w} \in \mathbb{R}^d$, then the following result holds due to the definition of **A-spectral** norm

$$\|\mathbf{B}\mathbf{w}\|_{\mathbf{A}} \leq \|\mathbf{B}\|_{\mathbf{A}} \|\mathbf{w}\|_{\mathbf{A}} \quad (29)$$

A.4 Characterization of the LS minimizer

By setting the gradient of (6) to zero and recalling the convexity of f_{LS} we immediately see that the minimizer of this objective is

$$\tilde{\mathbf{w}}^* := -\mathbf{S}^{-1}\mathbf{u}. \quad (30)$$

Indeed, one can easily verify that $\tilde{\mathbf{w}}^*$ is also an eigenvector of the matrix pair (\mathbf{B}, \mathbf{S}) since

$$\mathbf{B}\tilde{\mathbf{w}}^* = \mathbf{u}\mathbf{u}^\top(-\mathbf{S}^{-1}\mathbf{u}) = -\|\mathbf{u}\|_{\mathbf{S}^{-1}}^2\mathbf{u} = (\|\mathbf{u}\|_{\mathbf{S}^{-1}}^2)\mathbf{S}(-\mathbf{S}^{-1}\mathbf{u}) = \lambda_1\mathbf{S}\tilde{\mathbf{w}}^* \quad (31)$$

where $\lambda_1 := \|\mathbf{u}\|_{\mathbf{S}^{-1}}^2$ is the corresponding generalized eigenvalue. The associated eigenvector with λ_1 is

$$\mathbf{v}_1 := \tilde{\mathbf{w}}^*/\|\mathbf{u}\|_{\mathbf{S}^{-1}}. \quad (32)$$

Thereby we extend the normalized eigenvector to an \mathbf{S} -orthogonal basis $(\mathbf{v}_1, \mathbf{v}_2, \dots, \mathbf{v}_d)$ of \mathbb{R}^d such that

$$\langle \mathbf{v}_i, \mathbf{v}_j \rangle_{\mathbf{S}} = 0, \quad \forall i \neq j \quad \text{and} \quad \langle \mathbf{v}_i, \mathbf{v}_i \rangle_{\mathbf{S}} = \|\mathbf{v}_i\|_{\mathbf{S}} = 1, \quad \forall i \quad (33)$$

holds. Let $\mathbf{V}_2 := [\mathbf{v}_2, \mathbf{v}_3, \dots, \mathbf{v}_d]$ be the matrix whose $(i-1)$ -th column is $\mathbf{v}_i, i \in \{2, \dots, d\}$. The matrix \mathbf{B} is orthogonal to the matrix \mathbf{V}_2 since

$$\mathbf{B}\mathbf{V}_2 = \mathbf{u}\mathbf{u}^\top\mathbf{V}_2 = \mathbf{u}\mathbf{u}^\top\mathbf{S}^{-1}\mathbf{S}\mathbf{V}_2 \stackrel{(32)}{=} \|\mathbf{S}^{-1}\mathbf{u}\|_{\mathbf{S}}\mathbf{u} \underbrace{\left(\begin{array}{c} -\mathbf{v}_1^\top\mathbf{S}\mathbf{V}_2 \\ \mathbf{0} \end{array} \right)}_{\mathbf{0}}, \quad (34)$$

which is a zero matrix due to the \mathbf{A} -orthogonality of the basis (see Eq. (33)). As a result, the columns of \mathbf{V}_2 are eigenvectors associated with a zero eigenvalue. Since \mathbf{v}_1 and \mathbf{V}_2 form an \mathbf{S} -orthonormal basis of \mathbb{R}^d no further eigenvalues exist. We can conclude that any vector $\mathbf{w}^* \in \text{span}\{\mathbf{v}_1\}$ is a minimizer of the reparametrized ordinary least squares problem as presented in (8) and the minimum value of ρ relates to the eigenvalue as

$$\lambda_1 = -\min_{\mathbf{w}} \rho(\mathbf{w}).$$

Spectral representation of suboptimality Our convergence analysis is based on the angle between the current iterate \mathbf{w}_t and the leading eigenvector \mathbf{v}_1 , for which we recall property (P.1). We can express $\mathbf{w} \in \mathbb{R}^d$ in the \mathbf{S} -orthogonal basis that we defined above:

$$\mathbf{w} = \alpha_1\mathbf{v}_1 + \mathbf{V}_2\boldsymbol{\alpha}_2, \quad \alpha_1 \in \mathbb{R}, \quad \boldsymbol{\alpha}_2 \in \mathbb{R}^{d-1} \quad (35)$$

and since $\alpha_1\mathbf{v}_1$ is the \mathbf{S} -orthogonal projection of \mathbf{w} to $\text{span}\{\mathbf{v}_1\}$, the result of (P.2) implies

$$\cos^2 \angle_{\mathbf{S}}(\mathbf{w}, \mathbf{v}_1) = \frac{\|\alpha_1\mathbf{v}_1\|_{\mathbf{S}}^2}{\|\mathbf{w}\|_{\mathbf{S}}^2} = \frac{\alpha_1^2}{\|\mathbf{w}\|_{\mathbf{S}}^2}. \quad (36)$$

Clearly this metric is zero for the optimal solution \mathbf{v}_1 and else bounded by one from above. To justify it is a proper choice, the next proposition proves that suboptimality on ρ , i.e. $\rho(\mathbf{w}) - \rho(\mathbf{v}_1)$, relates directly to this angle.

Proposition 1. *The suboptimality of \mathbf{w} on $\rho(\mathbf{w})$ relates to $\sin^2 \angle_{\mathbf{S}}(\mathbf{w}, \mathbf{v}_1)$ as*

$$\rho(\mathbf{w}) - \rho(\mathbf{v}_1) = \lambda_1 \sin^2 \angle_{\mathbf{S}}(\mathbf{w}, \mathbf{v}_1), \quad (37)$$

where $\rho(\mathbf{v}_1) = \lambda_1$. This is equivalent to

$$\rho(\mathbf{w}) = -\lambda_1 \cos^2 \angle_{\mathbf{S}}(\mathbf{w}, \mathbf{v}_1). \quad (38)$$

Proof. We use the proposed eigenexpansion of Eq. (35) to rewrite

$$\mathbf{B}\mathbf{w} = (\alpha_1\mathbf{B}\mathbf{v}_1 + \mathbf{B}\mathbf{V}_2\boldsymbol{\alpha}_2) \stackrel{(34)}{=} \alpha_1\mathbf{B}\mathbf{v}_1 \stackrel{(31)}{=} \alpha_1\lambda_1\mathbf{S}\mathbf{v}_1 \quad (39)$$

and replace the above result into $\rho(\mathbf{w})$. Then

$$\rho(\mathbf{w}) = -\frac{\mathbf{w}^\top\mathbf{B}\mathbf{w}}{\mathbf{w}^\top\mathbf{S}\mathbf{w}} \stackrel{(39)}{=} -\alpha_1\lambda_1\frac{(\alpha_1\mathbf{v}_1 + \mathbf{V}_2\boldsymbol{\alpha}_2)^\top\mathbf{S}\mathbf{v}_1}{\|\mathbf{w}\|_{\mathbf{S}}^2} \stackrel{(33)}{=} -\lambda_1\frac{\alpha_1^2}{\|\mathbf{w}\|_{\mathbf{S}}^2} \stackrel{(36)}{=} -\lambda_1\cos^2\angle_{\mathbf{S}}(\mathbf{w}, \mathbf{v}_1),$$

which proves the second part of the proposition. The first follows directly from property (P.1). \square

Gradient-suboptimality connection Fermat's first-order optimality condition implies that the gradient is zero at the minimizer of $\rho(\mathbf{w})$. Considering the structure of $\rho(\mathbf{w})$, we propose a precise connection between the norm of gradient and suboptimality. Our analysis relies on the representation of the gradient $\nabla\rho(\mathbf{w})$ in the \mathbf{S} -orthonormal basis $\{\mathbf{v}_1, \dots, \mathbf{v}_d\}$ which is described in the next proposition.

Proposition 2. *Using the \mathbf{S} -orthogonal basis as given in Eq. (33), the gradient vector can be expanded as*

$$\|\mathbf{w}\|_{\mathbf{S}}^2\nabla\rho(\mathbf{w})/2 = -\lambda_1\alpha_1\sin^2\angle_{\mathbf{S}}(\mathbf{w}, \mathbf{v}_1)\mathbf{S}\mathbf{v}_1 + \lambda_1\cos^2\angle_{\mathbf{S}}(\mathbf{w}, \mathbf{v}_1)\mathbf{S}\mathbf{V}_2\boldsymbol{\alpha}_2 \quad (40)$$

Proof. The above derivation is based on two results: (i) \mathbf{v}_1 is an eigenvector of (\mathbf{B}, \mathbf{S}) and (ii) the representation of $\rho(\mathbf{w})$ in Proposition 1. We recall the definition of $\nabla\rho(\mathbf{w})$ in (18) and write

$$\begin{aligned} \nabla\rho(\mathbf{w})\|\mathbf{w}\|_{\mathbf{S}}^2/2 &= -\rho(\mathbf{w})\mathbf{S}\mathbf{w} - \mathbf{B}\mathbf{w} \\ &\stackrel{(39)}{=} -\rho(\mathbf{w})\mathbf{S}(\alpha_1\mathbf{v}_1 + \mathbf{V}_2\boldsymbol{\alpha}_2) + \lambda_1\alpha_1\mathbf{S}\mathbf{v}_1 \\ &\stackrel{(38)}{=} -(1 - \cos^2\angle_{\mathbf{S}}(\mathbf{w}, \mathbf{v}_1))\lambda_1\alpha_1\mathbf{S}\mathbf{v}_1 + \lambda_1\cos^2\angle_{\mathbf{S}}(\mathbf{w}, \mathbf{v}_1)\mathbf{S}\mathbf{V}_2\boldsymbol{\alpha}_2 \\ &= -\lambda_1\alpha_1\sin^2\angle_{\mathbf{S}}(\mathbf{w}, \mathbf{v}_1)\mathbf{S}\mathbf{v}_1 + \lambda_1\cos^2\angle_{\mathbf{S}}(\mathbf{w}, \mathbf{v}_1)\mathbf{S}\mathbf{V}_2\boldsymbol{\alpha}_2 \end{aligned}$$

\square

Exploiting the gradient representation of the last proposition, the next proposition establishes the connection between suboptimality and the \mathbf{S}^{-1} -norm of gradient $\nabla_{\mathbf{w}}\rho(\mathbf{w})$.

Proposition 3. *Suppose that $\rho(\mathbf{w}) \neq 0$, then the \mathbf{S}^{-1} -norm of the gradient $\nabla\rho(\mathbf{w})$ relates to the suboptimality as*

$$\|\mathbf{w}\|_{\mathbf{S}}^2\|\nabla\rho(\mathbf{w})\|_{\mathbf{S}^{-1}}^2/(4|\rho(\mathbf{w})|) = \rho(\mathbf{w}) - \rho(\mathbf{v}_1) \quad (41)$$

Proof. Multiplying the gradient representation in Proposition 2 by \mathbf{S}^{-1} yields

$$\mathbf{S}^{-1}\nabla\rho(\mathbf{w})\|\mathbf{w}\|_{\mathbf{S}}^2/2 = -\lambda_1\alpha_1\sin^2\angle_{\mathbf{S}}(\mathbf{w}, \mathbf{v}_1)\mathbf{v}_1 + \lambda_1\cos^2\angle_{\mathbf{S}}(\mathbf{w}, \mathbf{v}_1)\mathbf{V}_2\boldsymbol{\alpha}_2.$$

By combining the above result with the \mathbf{S} -orthogonality of the basis $(\mathbf{v}_1, \mathbf{V}_2)$, we derive the (squared) \mathbf{S}^{-1} -norm of the gradient as

$$\begin{aligned} \nabla\rho(\mathbf{w})^\top\mathbf{S}^{-1}\nabla\rho(\mathbf{w})/4 &\stackrel{(33)}{=} T_1 + T_2 \\ T_1 &:= \|\mathbf{w}\|_{\mathbf{S}}^{-4}\lambda_1^2\alpha_1^2\sin^4\angle_{\mathbf{S}}(\mathbf{w}, \mathbf{v}_1), \quad T_2 := \|\mathbf{w}\|_{\mathbf{S}}^{-4}\lambda_1^2\cos^4\angle_{\mathbf{S}}(\mathbf{w}, \mathbf{v}_1)\|\boldsymbol{\alpha}_2\|^2. \end{aligned} \quad (42)$$

It remains to simplify the terms T_1 and T_2 . For T_1 ,

$$\|\mathbf{w}\|_{\mathbf{S}}^2T_1/(\lambda_1^2\sin^4\angle_{\mathbf{S}}(\mathbf{w}, \mathbf{v}_1)) = \|\mathbf{w}\|_{\mathbf{S}}^{-2}\alpha_1^2 \stackrel{(36)}{=} \cos^2\angle_{\mathbf{S}}(\mathbf{w}, \mathbf{v}_1).$$

Similarly, we simplify T_2 :

$$\begin{aligned}
\|\mathbf{w}\|_{\mathbf{S}}^2 T_2 / (\lambda_1^2 \cos^4 \angle_{\mathbf{S}}(\mathbf{w}, \mathbf{v}_1)) &= \|\mathbf{w}\|_{\mathbf{S}}^{-2} \|\alpha_2\|^2 \\
&= \|\mathbf{w}\|_{\mathbf{S}}^{-2} (\|\mathbf{w}\|_{\mathbf{S}}^2 - \alpha_1^2) \\
&= 1 - \frac{\alpha_1^2}{\|\mathbf{w}\|_{\mathbf{S}}^2} \\
&\stackrel{(36)}{=} 1 - \cos^2 \angle_{\mathbf{S}}(\mathbf{w}, \mathbf{v}_1) \\
&= \sin^2 \angle_{\mathbf{S}}(\mathbf{w}, \mathbf{v}_1)
\end{aligned}$$

Replacing the simplified expression of T_1 and T_2 into Eq. (42) yields

$$\begin{aligned}
\|\mathbf{w}\|_{\mathbf{S}}^2 \|\nabla_{\mathbf{w}} \rho(\mathbf{w})\|_{\mathbf{S}^{-1}}^2 / 4 &= \lambda_1^2 \cos^2 \angle_{\mathbf{S}}(\mathbf{w}, \mathbf{v}_1) \sin^2 \angle_{\mathbf{S}}(\mathbf{w}, \mathbf{v}_1) (\sin^2 \angle_{\mathbf{S}}(\mathbf{w}, \mathbf{v}_1) + \cos^2 \angle_{\mathbf{S}}(\mathbf{w}, \mathbf{v}_1)) \\
&= \lambda_1^2 \cos^2 \angle_{\mathbf{S}}(\mathbf{w}, \mathbf{v}_1) \sin^2 \angle_{\mathbf{S}}(\mathbf{w}, \mathbf{v}_1), \\
&\stackrel{(38)}{=} |\rho(\mathbf{w})| \lambda_1 \|\sin^2 \angle_{\mathbf{S}}(\mathbf{w}, \mathbf{v}_1)\| \\
&\stackrel{(37)}{=} |\rho(\mathbf{w})| (\rho(\mathbf{w}) - \rho(\mathbf{v}_1)).
\end{aligned}$$

A rearrangement of terms in the above equation concludes the proof. \square

A.5 Convergence proof

We have seen: suboptimality in $\rho(\mathbf{w})$ directly relates to $\sin^2 \angle_{\mathbf{S}}(\mathbf{w}, \mathbf{v}_1)$ for all $\mathbf{w} \setminus \{\mathbf{0}\}$. In the next lemma we prove that this quantity is strictly decreased by repeated GD updates at a linear rate.

Lemma 3. *Suppose that Assumption 1 holds and consider GD (GD) steps on (8) with stepsize $\eta_t = \frac{\|\mathbf{w}_t\|_{\mathbf{S}}^2}{2L|\rho(\mathbf{w}_t)|}$. Then, for any $\mathbf{w}_0 \in \mathbb{R}^d$ such that $\rho(\mathbf{w}_0) < 0$, the updates of Eq. (17) yield the following linear convergence rate*

$$\sin^2 \angle_{\mathbf{S}}(\mathbf{w}_t, \mathbf{v}_1) \leq \left(1 - \frac{\mu}{L}\right)^{2t} \sin^2 \angle_{\mathbf{S}}(\mathbf{w}_0, \mathbf{v}_1) \quad (43)$$

Proof. To prove the above statement, we relate the sine of the angle of a given iterate \mathbf{w}_{t+1} with \mathbf{v}_1 in terms of the previous angle $\angle(\mathbf{w}_t, \mathbf{v}_1)$. Towards this end, we assume for the moment that $\rho(\mathbf{w}_t) \neq 0$ but note that this naturally always holds whenever $\rho(\mathbf{w}_0) \neq 0$,⁵ such that the angle relation can be recursively applied through all $t \geq 0$ to yield Eq. (43).

(i) We start by deriving an expression for $\sin \angle_{\mathbf{S}}(\mathbf{v}_1, \mathbf{w}_t)$. By (24) and the definition $\rho(\mathbf{w}_t)$, we have that $-\rho(\mathbf{w}_t)\mathbf{w}_t$ is the \mathbf{S} -orthogonal projection of $\mathbf{S}^{-1}\mathbf{B}\mathbf{w}_t$ to $\text{span}\{\mathbf{w}_t\}$. Indeed,

$$\langle \mathbf{S}^{-1}\mathbf{B}\mathbf{w}_t + \rho(\mathbf{w}_t)\mathbf{w}_t, \mathbf{w}_t \rangle_{\mathbf{S}} = \mathbf{w}_t^{\top} \mathbf{B} \mathbf{S}^{-1} \mathbf{S} \mathbf{w}_t - \frac{\mathbf{w}_t^{\top} \mathbf{B} \mathbf{w}_t}{\mathbf{w}_t^{\top} \mathbf{S} \mathbf{w}_t} \mathbf{w}_t^{\top} \mathbf{S} \mathbf{w}_t = 0.$$

Note that $\mathbf{S}^{-1}\mathbf{B}\mathbf{w}_t = (\mathbf{S}^{-1}\mathbf{u})(\mathbf{u}^{\top}\mathbf{w}_t)$ is a nonzero multiple of \mathbf{v}_1 and thus $\sin \angle_{\mathbf{S}}(\mathbf{S}^{-1}\mathbf{B}\mathbf{w}_t, \mathbf{w}_t) = \sin \angle_{\mathbf{S}}(\mathbf{v}_1, \mathbf{w}_t)$.

Thus, by (P.2) we have

$$\sin \angle_{\mathbf{S}}(\mathbf{v}_1, \mathbf{w}_t) = \sin \angle_{\mathbf{S}}(\mathbf{S}^{-1}\mathbf{B}\mathbf{w}_t, \mathbf{w}_t) = \frac{\|\mathbf{S}^{-1}\mathbf{B}\mathbf{w}_t + \rho(\mathbf{w}_t)\mathbf{w}_t\|_{\mathbf{S}}}{\|\mathbf{S}^{-1}\mathbf{B}\mathbf{w}_t\|_{\mathbf{S}}}. \quad (44)$$

⁵as we will show later by induction.

(ii) We now derive an expression for $\sin \angle_{\mathbf{S}}(\mathbf{v}_1, \mathbf{w}_{t+1})$. Let $a_{t+1} \in \mathbb{R}$ such that $a_{t+1}\mathbf{w}_{t+1} \in \mathbb{R}^d$ is the \mathbf{S} -orthogonal projection of $\mathbf{S}^{-1}\mathbf{B}\mathbf{w}_t$ to $\text{span}\{\mathbf{w}_{t+1}\}$. Then

$$\begin{aligned} \langle \mathbf{S}^{-1}\mathbf{B}\mathbf{w}_t - a_{t+1}\mathbf{w}_{t+1}, \mathbf{w}_{t+1} \rangle_{\mathbf{S}} &= 0 \\ \Rightarrow \langle \mathbf{S}^{-1}\mathbf{B}\mathbf{w}_t - a_{t+1}\mathbf{w}_{t+1}, (a_{t+1} + \rho(\mathbf{w}_t))\mathbf{w}_{t+1} \rangle_{\mathbf{S}} &= 0. \end{aligned} \quad (45)$$

By the Pythagorean theorem and (45), we get

$$\begin{aligned} \|\mathbf{S}^{-1}\mathbf{B}\mathbf{w}_t + \rho(\mathbf{w}_t)\mathbf{w}_{t+1}\|_{\mathbf{S}}^2 &= \|\mathbf{S}^{-1}\mathbf{B}\mathbf{w}_t - a_{t+1}\mathbf{w}_{t+1}\|_{\mathbf{S}}^2 + \|(a_{t+1} + \rho(\mathbf{w}_t))\mathbf{w}_{t+1}\|_{\mathbf{S}}^2 \\ &\geq \|\mathbf{S}^{-1}\mathbf{B}\mathbf{w}_t - a_{t+1}\mathbf{w}_{t+1}\|_{\mathbf{S}}^2. \end{aligned} \quad (46)$$

Hence, again by (P.2)

$$\begin{aligned} \sin \angle_{\mathbf{S}}(\mathbf{v}_1, \mathbf{w}_{t+1}) &= \sin \angle_{\mathbf{S}}(\mathbf{S}^{-1}\mathbf{B}\mathbf{w}_t, \mathbf{w}_{t+1}) = \frac{\|\mathbf{S}^{-1}\mathbf{B}\mathbf{w}_t - a_{t+1}\mathbf{w}_{t+1}\|_{\mathbf{S}}}{\|\mathbf{S}^{-1}\mathbf{B}\mathbf{w}_t\|_{\mathbf{S}}} \\ &\stackrel{(46)}{\leq} \frac{\|\mathbf{S}^{-1}\mathbf{B}\mathbf{w}_t + \rho(\mathbf{w}_t)\mathbf{w}_{t+1}\|_{\mathbf{S}}}{\|\mathbf{S}^{-1}\mathbf{B}\mathbf{w}_t\|_{\mathbf{S}}}. \end{aligned} \quad (47)$$

(iii) To see how the two quantities on the right hand side of (44) and (47) relate, let us rewrite the GD updates from Eq. (17) as follows

$$\begin{aligned} \rho(\mathbf{w}_t)\mathbf{w}_{t+1} &= \rho(\mathbf{w}_t)\mathbf{w}_t - \frac{\mathbf{S}}{L}(\mathbf{S}^{-1}\mathbf{B}\mathbf{w}_t + \rho(\mathbf{w}_t)\mathbf{w}_t) \\ \Leftrightarrow \mathbf{S}^{-1}\mathbf{B}\mathbf{w}_t + \rho(\mathbf{w}_t)\mathbf{w}_{t+1} &= \mathbf{S}^{-1}\mathbf{B}\mathbf{w}_t + \rho(\mathbf{w}_t)\mathbf{w}_t - \frac{\mathbf{S}}{L}(\mathbf{S}^{-1}\mathbf{B}\mathbf{w}_t + \rho(\mathbf{w}_t)\mathbf{w}_t) \\ \Leftrightarrow \mathbf{S}^{-1}\mathbf{B}\mathbf{w}_t + \rho(\mathbf{w}_t)\mathbf{w}_{t+1} &= \left(\mathbf{I} - \frac{\mathbf{S}}{L}\right)(\mathbf{S}^{-1}\mathbf{B}\mathbf{w}_t + \rho(\mathbf{w}_t)\mathbf{w}_t). \end{aligned} \quad (48)$$

By taking the \mathbf{S} -norm we can conclude

$$\begin{aligned} \|\mathbf{S}^{-1}\mathbf{B}\mathbf{w}_t + \rho(\mathbf{w}_t)\mathbf{w}_{t+1}\|_{\mathbf{S}} &\stackrel{(48)}{\leq} \left\|\mathbf{I} - \frac{\mathbf{S}}{L}\right\|_{\mathbf{S}} \cdot \|\mathbf{S}^{-1}\mathbf{B}\mathbf{w}_t + \rho(\mathbf{w}_t)\mathbf{w}_t\|_{\mathbf{S}} \\ &\leq \left(1 - \frac{\mu}{L}\right) \|\mathbf{S}^{-1}\mathbf{B}\mathbf{w}_t + \rho(\mathbf{w}_t)\mathbf{w}_t\|_{\mathbf{S}}, \end{aligned} \quad (49)$$

where the first inequality is due to property (P.4) of the \mathbf{S} -spectral norm and the second is due to Assumption (1) and (P.3), which allows us to bound the latter in term of the usual spectral norm as follows

$$\|\mathbf{I} - \mathbf{S}/L\|_{\mathbf{S}} \stackrel{(P.3)}{=} \|\mathbf{S}^{1/2}(\mathbf{I} - \mathbf{S}/L)\mathbf{S}^{-1/2}\|_2 = \|\mathbf{I} - \mathbf{S}/L\|_2 \stackrel{(2)}{\leq} 1 - \mu/L. \quad (50)$$

(iv) Combining the above results yields the desired bound

$$\begin{aligned} \sin \angle_{\mathbf{S}}(\mathbf{v}_1, \mathbf{w}_{t+1}) &\stackrel{(47)}{\leq} \frac{\|\mathbf{S}^{-1}\mathbf{B}\mathbf{w}_t + \rho(\mathbf{w}_t)\mathbf{w}_{t+1}\|_{\mathbf{S}}}{\|\mathbf{S}^{-1}\mathbf{B}\mathbf{w}_t\|_{\mathbf{S}}} \\ &\stackrel{(49)}{\leq} \left(1 - \frac{\mu}{L}\right) \frac{\|\mathbf{S}^{-1}\mathbf{B}\mathbf{w}_t + \rho(\mathbf{w}_t)\mathbf{w}_t\|_{\mathbf{S}}}{\|\mathbf{S}^{-1}\mathbf{B}\mathbf{w}_t\|_{\mathbf{S}}} \\ &\stackrel{(44)}{=} \left(1 - \frac{\mu}{L}\right) \sin \angle_{\mathbf{S}}(\mathbf{v}_1, \mathbf{w}_t). \end{aligned} \quad (51)$$

(v) Finally, we show that the initially made assumption $\rho(\mathbf{w}_t) \neq 0$ is naturally satisfied in all iterations. First, $\rho(\mathbf{w}_0) < 0$ by assumption. Second, assuming $\rho(\mathbf{w}_{\hat{t}}) < 0$ for an arbitrary $\hat{t} \in \mathbb{N}^+$ gives that the above analysis (i-iv) holds for $\hat{t} + 1$ and thus (51) together with (37) and the fact that $\lambda_1 > 0$ give

$$\rho(\mathbf{w}_{\hat{t}+1}) = -\lambda_1(1 - \sin^2(\mathbf{v}_1, \mathbf{w}_{\hat{t}+1})) < -\lambda_1(1 - \sin^2(\mathbf{v}_1, \mathbf{w}_{\hat{t}})) = \rho(\mathbf{w}_{\hat{t}}) < 0,$$

where the last inequality is our induction hypothesis. Thus $\rho(\mathbf{w}_{t+1}) < 0$ and we can conclude by induction that $\rho(\mathbf{w}_t) < 0, \forall t \in \mathbb{N}^+$.

As a result, (51) holds $\forall t \in \mathbb{N}^+$, which (applied recursively) proves the statement (43). \square

We are now ready to prove Theorem 1.

Proof of Theorem (1): By combining the results of Lemma 3 as well as Proposition 1 and 3, we can complete the proof of the Theorem 1 as follows

$$\begin{aligned} \|\mathbf{w}_t\|_{\mathbf{S}}^2 \|\nabla_{\mathbf{w}} \rho(\mathbf{w}_t)\|_{\mathbf{S}^{-1}}^2 / |4\rho(\mathbf{w}_t)| &\stackrel{(41)}{=} (\rho(\mathbf{w}_t) - \rho(\mathbf{w}^*)) \\ &\stackrel{(37)}{=} \lambda_1 \sin^2 \angle_{\mathbf{S}}(\mathbf{w}_t, \mathbf{v}_1) \\ &\stackrel{(43)}{\leq} \left(1 - \frac{\mu}{L}\right)^{2t} \lambda_1 \sin^2 \angle_{\mathbf{S}}(\mathbf{w}_0, \mathbf{v}_1) \\ &\stackrel{(37)}{=} \left(1 - \frac{\mu}{L}\right)^{2t} (\rho(\mathbf{w}_0) - \rho(\mathbf{w}^*)). \end{aligned}$$

B Learning half-spaces

In this section, we provide a convergence analysis for Algorithm 1 on the problem of learning halfspaces

$$\min_{\tilde{\mathbf{w}} \in \mathbb{R}^d} (f_{\text{LH}}(\tilde{\mathbf{w}}) := \mathbf{E}_{y, \mathbf{x}} [\varphi(-y\mathbf{x}^\top \tilde{\mathbf{w}})] = \mathbf{E}_{\mathbf{z}} [\varphi(\mathbf{z}^\top \tilde{\mathbf{w}})]). \quad (12 \text{ revisited})$$

As before, we reparametrize $\tilde{\mathbf{w}}$ by means of the covariance matrix \mathbf{S} as

$$\tilde{\mathbf{w}} := g\mathbf{w} / \|\mathbf{w}\|_{\mathbf{S}}. \quad (4 \text{ revisited})$$

We assume that the domain of $f_{\text{LH}}(\tilde{\mathbf{w}})$ is \mathbb{R}^d but exclude $\mathbf{0}$ such that (4) is always well defined. Thus, the domain of the new parameterization is $(\mathbf{w}, g) \in (\mathbb{R}^d \setminus \{\mathbf{0}\}) \otimes \mathbb{R} \subset \mathbb{R}^{d+1}$.

B.1 Preliminaries

Recall the normality assumption on the data distribution.

Assumption 2. *[Normality assumption on data distribution] We assume that \mathbf{z} is a multivariate normal random variable distributed as $\mathbf{z} \sim \mathcal{N}(\mathbf{u}, \mathbf{S})$.*

Under the above assumption we have that for a differentiable function $g(\mathbf{z}) : \mathbb{R}^d \rightarrow \mathbb{R}$ the following equality holds

$$\mathbf{E}_{\mathbf{z}} [g(\mathbf{z})\mathbf{z}] = \mathbf{E}_{\mathbf{z}} [g(\mathbf{z})] \mathbf{u} + \mathbf{S} \mathbf{E}_{\mathbf{z}} [\nabla_{\mathbf{z}} g(\mathbf{z})]. \quad (52)$$

This result, which can be derived using a simple application of integration by parts, is called *Stein's lemma* [20]. In the next lemma, we show that this allows us to simplify the expression of the gradient of Eq. 12.

Lemma 4 (restated result from [10]). *Under the normality assumption on the data distribution (Assumption 2), the gradient of Eq. 12 can be expressed as*

$$\nabla_{\tilde{\mathbf{w}}} f_{\text{LH}}(\tilde{\mathbf{w}}) = c_1(\tilde{\mathbf{w}})\mathbf{u} + c_2(\tilde{\mathbf{w}})\mathbf{S}\tilde{\mathbf{w}},$$

where $c_i \in \mathbb{R}$ depends on the i -th derivative of the loss function denoted by $\varphi^{(i)}$ as

$$c_i(\tilde{\mathbf{w}}) = \mathbf{E}_{\mathbf{z}} \left[\varphi^{(i)}(\mathbf{z}^\top \tilde{\mathbf{w}}) \right].$$

Proof. The result follows from a straight forward application of Stein’s lemma (Eq. (52)). See detailed derivation in [10]. \square

In addition to the assumption on the data distribution, the proposed analysis also requires a rather weak assumptions on f_{LH} and loss function φ .

Assumption 3. *[Assumptions on loss function]* We assume that the loss function $\varphi : \mathbb{R} \rightarrow \mathbb{R}$ is infinitely differentiable, i.e. $\varphi \in C^\infty(\mathbb{R}, \mathbb{R})$, with a bounded derivative, i.e. $\exists \Phi > 0$ such that $|\varphi^{(1)}(\beta)| \leq \Phi, \forall \beta \in \mathbb{R}$.

Assumption 4. *[Smoothness assumption]* We assume that the objective $f : \mathbb{R}^d \rightarrow \mathbb{R}$ is ζ -smooth if it is differentiable on \mathbb{R} and its gradient is ζ -Lipschitz. Furthermore, we assume that a solution $\alpha^* := \arg \min_{\alpha} \|\nabla f(\alpha \mathbf{w})\|^2$ exists that is bounded in the sense that $\forall \mathbf{w} \in \mathbb{R}^d, -\infty < \alpha^* < \infty$.⁶

Recall that ζ -smoothness of f_{LH} , which is mentioned in the last assumption, implies that the gradient of f_{LH} is ζ -Lipschitz, i.e.

$$\|\nabla f_{\text{LH}}(\tilde{\mathbf{w}}_1) - \nabla f_{\text{LH}}(\tilde{\mathbf{w}}_2)\| \leq \zeta \|\tilde{\mathbf{w}}_1 - \tilde{\mathbf{w}}_2\|. \quad (53)$$

B.2 Global characterization

Here, we prove a result about a global property of the solution of the problem of learning halfspaces.

Lemma 1. *Under Assumptions 1 and 2, all bounded critical points $\tilde{\mathbf{w}}_*$ of f_{LH} have the general form*

$$\tilde{\mathbf{w}}_* = g_* \mathbf{S}^{-1} \mathbf{u},$$

where the scalar $g_* \in \mathbb{R}$ depends on $\tilde{\mathbf{w}}_*$ and the choice of the loss function φ .

Proof. Setting the gradient of the objective (12) (see derivation in Lemma 4) to zero concludes the result. \square

B.3 Established Convergence Rate

Based on this assumption, we derive a linear convergence rate for GDNP presented in Algorithm 1. We first restate the convergence guarantee before providing a detailed proof.

Theorem 4. *[Convergence rate of GDNP on learning halfspaces]* Suppose Assumptions 1– 4 hold. Let $\tilde{\mathbf{w}}_{T_d}$ be the output of GDNP on f_{LH} with the following choice of stepsizes

$$s_t := s(\mathbf{w}_t, g_t) = -\|\mathbf{w}_t\|_{\mathbf{S}}^3 / (L g_t h(\mathbf{w}_t, g_t) \mathbf{u}^\top \mathbf{w}_t), \quad t = 1, \dots, T_d, \quad (54)$$

where $h(\mathbf{w}_t, g_t) = \mathbf{E}_{\mathbf{z}} [\varphi'(g_t \mathbf{z}^\top \mathbf{w}_t / \|\mathbf{w}_t\|_{\mathbf{S}})] \neq 0$ is a stopping criterion. If $\rho(\mathbf{w}_0) \neq 0$ (see Eq. (8)), then $\tilde{\mathbf{w}}_{T_d}$ is an approximate critical point of f_{LH} in the sense that

$$\|\nabla_{\tilde{\mathbf{w}}} f(\tilde{\mathbf{w}}_{T_d})\|^2 \leq (1 - \mu/L)^{2T_d} \Phi^2 (\rho(\mathbf{w}_0) - \rho^*) + 2^{-T_d} \zeta |b_t^{(0)} - a_t^{(0)}| / \mu^2. \quad (55)$$

⁶This is a rather technical but not so restrictive assumption. For example for the sigmoid loss it always holds unless the classification error of \mathbf{w} is already zero.

B.3.1 Proof sketch

As mentioned earlier, the objective f_{LH} on Gaussian inputs has a particular *global* property. Namely, all its critical points are aligned along the same direction. The key idea is that \mathbf{S} -reparameterization provides this global information to a local optimization method through an elegant length-direction decoupling. This allows GDNP to mimic the behaviour of Gradient Descent on the above mentioned Rayleigh quotient for the directional updates and thereby inherit the linear convergence rate. At the same time, the scaling factor can easily be brought to a critical point by a fast, one dimensional search algorithm. We formalize and combine these intuitions in a detailed proof below.

B.3.2 Gradient in the normalized parameterization

Since GDNP relies on the normalized parameterization, we first need to derive the gradient of the objective in this parameterization

$$\min_{\mathbf{w}, g} \left(f_{\text{LH}}(\mathbf{w}, g) := \mathbf{E}_{\mathbf{z}} \left[\varphi \left(g \frac{\mathbf{z}^\top \mathbf{w}}{\|\mathbf{w}\|_{\mathbf{S}}} \right) \right] \right). \quad (56)$$

Straight forward calculations yields the following connection between the gradient formulation in the original parameterization $\nabla_{\tilde{\mathbf{w}}} f_{\text{LH}} = \mathbf{E}_{\mathbf{z}}[\varphi^{(1)}(\tilde{\mathbf{w}}^\top \mathbf{z})\mathbf{z}]$ and the gradient in the normalized parameterization

$$\nabla_{\mathbf{w}} f_{\text{LH}}(\mathbf{w}, g) = g \mathbf{A}_{\mathbf{w}} \nabla_{\tilde{\mathbf{w}}} f_{\text{LH}}(\tilde{\mathbf{w}}), \quad \partial_g f_{\text{LH}}(\mathbf{w}, g) = \mathbf{w}^\top \nabla_{\tilde{\mathbf{w}}} f_{\text{LH}}(\tilde{\mathbf{w}}) / \|\mathbf{w}\|_{\mathbf{S}} \quad (57)$$

where

$$\mathbf{A}_{\mathbf{w}} := \mathbf{I} / \|\mathbf{w}\|_{\mathbf{S}} - \mathbf{S} \mathbf{w} \mathbf{w}^\top / \|\mathbf{w}\|_{\mathbf{S}}^3.$$

Note that the vector $\mathbf{S} \mathbf{w}$ is orthogonal to the column space of $\mathbf{A}_{\mathbf{w}}$ since

$$\mathbf{A}_{\mathbf{w}} \mathbf{S} \mathbf{w} = \left(\mathbf{S} \mathbf{w} - \frac{\|\mathbf{w}\|_{\mathbf{S}}^2}{\|\mathbf{w}\|_{\mathbf{S}}^2} \mathbf{S} \mathbf{w} \right) / \|\mathbf{w}\|_{\mathbf{S}} = 0. \quad (58)$$

We will repeatedly use the above property in our future analysis. In the next lemma, we establish a connection between the norm of gradients in different parameterizations.

Proposition 4. *Under the reparameterization (4), the following holds:*

$$\|\nabla_{\tilde{\mathbf{w}}} f(\tilde{\mathbf{w}})\|_{\mathbf{S}^{-1}}^2 = \|\mathbf{w}\|_{\mathbf{S}}^2 \|\nabla_{\mathbf{w}} f(\mathbf{w}, g)\|_{\mathbf{S}^{-1}}^2 / g^2 + (\partial_g f(\mathbf{w}, g))^2 \quad (59)$$

Proof. We introduce the vector $\mathbf{q}_1 = \mathbf{S} \mathbf{w} / \|\mathbf{w}\|_{\mathbf{S}}$ that has unit \mathbf{S}^{-1} -norm, i.e. $\|\mathbf{q}_1\|_{\mathbf{S}^{-1}} = 1$.

According to Eq. (58),

$$\mathbf{A}_{\mathbf{w}} \mathbf{q}_1 = 0$$

holds. Now, we extend this vector to an \mathbf{S}^{-1} -orthogonal basis $\{\mathbf{q}_1, \mathbf{q}_2, \dots, \mathbf{q}_d\}$ of \mathbb{R}^d such that

$$\langle \mathbf{q}_i, \mathbf{q}_i \rangle_{\mathbf{S}^{-1}} = 1, \quad \forall i \text{ and } \langle \mathbf{q}_i, \mathbf{q}_j \rangle_{\mathbf{S}^{-1}} = 0, \quad \forall i \neq j.$$

Let \mathbf{Q}_2 be a matrix whose columns are $\{\mathbf{q}_2, \dots, \mathbf{q}_d\}$. The choice of \mathbf{q}_1 together with \mathbf{S}^{-1} -orthogonality of the basis imply that \mathbf{w} is orthogonal to \mathbf{Q}_2 :

$$\mathbf{w}^\top \mathbf{q}_j = \|\mathbf{w}\|_{\mathbf{S}} \langle \mathbf{q}_1, \mathbf{q}_j \rangle_{\mathbf{S}^{-1}} = 0, \quad \forall j \neq 1$$

Consider the gradient expansion in the new basis, i.e.

$$\nabla_{\tilde{\mathbf{w}}} f(\tilde{\mathbf{w}}) = \alpha_1 \mathbf{q}_1 + \mathbf{Q}_2 \alpha_2, \quad \|\nabla_{\tilde{\mathbf{w}}} f(\tilde{\mathbf{w}})\|_{\mathbf{S}^{-1}}^2 = \alpha_1^2 + \|\alpha_2\|_2^2$$

Plugging the above expansion into Eq. (57) yields

$$\nabla_{\mathbf{w}} f(\mathbf{w}, g) = g \mathbf{Q}_2 \boldsymbol{\alpha}_2 / \|\mathbf{w}\|_{\mathbf{S}}, \quad \partial_g f(\mathbf{w}, g) = \alpha_1 \quad (60)$$

hence the \mathbf{S}^{-1} -norm of the directional gradient in the new parameterization is

$$\|\nabla_{\mathbf{w}} f(\mathbf{w}, g)\|_{\mathbf{S}^{-1}}^2 = g^2 \|\boldsymbol{\alpha}_2\|_2^2 / \|\mathbf{w}\|_{\mathbf{S}}^2 \quad (61)$$

Therefore, one can establish the following connection between the \mathbf{S}^{-1} -norm of gradient in the two different parameterizations:

$$\begin{aligned} \|\nabla_{\tilde{\mathbf{w}}} f(\tilde{\mathbf{w}})\|_{\mathbf{S}^{-1}}^2 &= \alpha_1^2 + \|\boldsymbol{\alpha}_2\|_2^2 \\ &\stackrel{(60)}{=} (\partial_g f(\mathbf{w}, g))^2 + \|\boldsymbol{\alpha}_2\|_2^2 \\ &\stackrel{(61)}{=} (\partial_g f(\mathbf{w}, g))^2 + \|\mathbf{w}\|_{\mathbf{S}}^2 \|\nabla_{\mathbf{w}} f(\mathbf{w}, g)\|_{\mathbf{S}^{-1}}^2 / g^2 \end{aligned}$$

□

The above lemma allows us to first analyze convergence in the (\mathbf{w}, g) -parameterization and then we relate the result to the original $\tilde{\mathbf{w}}$ -parameterization in the following way: Given that the iterates $\{\mathbf{w}_t, g_t\}_{t \in \mathbb{N}^+}$ converge to a critical point of $f_{\text{LH}}(\mathbf{w}, g)$, one can use Eq. (60) to prove that $\tilde{\mathbf{w}}_t = g_t \mathbf{w}_t / \|\mathbf{w}_t\|_{\mathbf{S}}$ also converges to a critical point of $f_{\text{LH}}(\tilde{\mathbf{w}})$.

For the particular case of learning halfspaces with Gaussian input, the result of Lemma 4 allows us to write the gradient ∇f_{LH} as

$$\nabla_{\tilde{\mathbf{w}}} f_{\text{LH}}(\tilde{\mathbf{w}}) = c_1(\tilde{\mathbf{w}}) \mathbf{u} + c_2(\tilde{\mathbf{w}}) \mathbf{S} \tilde{\mathbf{w}},$$

where the constants c_1 and c_2 are determined by the choice of the loss. Replacing this expression in Eq. (57) yields the following formulation for the gradient in normalized coordinates

$$\nabla_{\mathbf{w}} f_{\text{LH}}(\mathbf{w}) = g c_1(\mathbf{w}, g) \mathbf{A}_{\mathbf{w}} \mathbf{u} + g c_2(\mathbf{w}, g) \mathbf{A}_{\mathbf{w}} \mathbf{S} \mathbf{w}, \quad (62)$$

where $c_i(\mathbf{w}, g) = c_i(\tilde{\mathbf{w}}(\mathbf{w}, g))$. Yet, due to the specific matrix $\mathbf{A}_{\mathbf{w}}$ that arises when reparametrizing according to (4), the vector $\mathbf{S} \mathbf{w}$ is again in the kernel of $\mathbf{A}_{\mathbf{w}}$ (see Eq. (58)) and hence

$$\nabla_{\mathbf{w}} f_{\text{LH}}(\mathbf{w}) = g c_1(\mathbf{w}, g) \mathbf{A}_{\mathbf{w}} \mathbf{u}. \quad (63)$$

B.3.3 Convergence of the scalar g

Lemma 5 (Convergence of scalar). *Under assumptions of theorem 4, in each iteration $t \in \mathbb{N}^+$ of GDNP (Algorithm 1) the partial derivative of f_{LH} as in Eq. (56) converges to zero at the following linear rate*

$$\left(\partial_g f_{\text{LH}}(\mathbf{w}_t, a_t^{(T_s)}) \right)^2 \leq 2^{-T_s} \zeta |b_t^{(0)} - a_t^{(0)}| / \mu^2 \quad (64)$$

Proof. According to Algorithm 1, the length of the search space for g is cut in half by each bisection step and thus reduces to

$$|a_t^{(T_s)} - b_t^{(T_s)}| \leq 2^{-T_s} |b_t^{(0)} - a_t^{(0)}|$$

after T_s iterations. The continuity of $\partial_g f_{\text{LH}}$ given by Assumption 4 and the fact that Algorithm 1 guarantees $\partial_g f_{\text{LH}}(\mathbf{w}_t, a_t^{(m)}) \cdot \partial_g f_{\text{LH}}(\mathbf{w}_t, b_t^{(m)}) < 0$, $\forall m \in \mathbb{N}^+$ allow us to conclude that there exists a root g^* for $\partial_g f_{\text{LH}}$ between $a_t^{(T_s)}$ and $b_t^{(T_s)}$ for which

$$|a_t^{(T_s)} - g^*| \leq 2^{-T_s} |b_t^{(0)} - a_t^{(0)}|$$

holds.

The next step is to relate the above distance to the partial derivative of $f_{\text{LH}}(\mathbf{w}, g)$ w.r.t g . Consider the compact notation $\mathbf{w}'_t = \mathbf{w}_t / \|\mathbf{w}_t\|_{\mathbf{S}}$. Using this notation and the gradient expression in Eq. (57), the difference of partial derivatives can be written as

$$\begin{aligned} \left(\partial_g f_{\text{LH}}(\mathbf{w}_t, a_t^{(T_s)})\right)^2 &= \left(\partial_g f_{\text{LH}}(\mathbf{w}_t, a_t^{(T_s)}) - \partial_g f_{\text{LH}}(\mathbf{w}_t, g^*)\right)^2 \\ &= \left(\left(\nabla_{\tilde{\mathbf{w}}} f_{\text{LH}}(a_t^{(T_s)} \mathbf{w}'_t) - \nabla_{\tilde{\mathbf{w}}} f_{\text{LH}}(g^* \mathbf{w}'_t)\right)^\top \mathbf{w}'_t\right)^2. \end{aligned} \quad (65)$$

Using the smoothness assumption on f_{LH} we bound the above difference as follows

$$\begin{aligned} \left(\left(\nabla_{\tilde{\mathbf{w}}} f_{\text{LH}}(a_t^{(T_s)} \mathbf{w}'_t) - \nabla_{\tilde{\mathbf{w}}} f_{\text{LH}}(g^* \mathbf{w}'_t)\right)^\top \mathbf{w}'_t\right)^2 &\leq \|\mathbf{w}'_t\|^2 \|\nabla_{\tilde{\mathbf{w}}} f_{\text{LH}}(a_t^{(T_s)} \mathbf{w}'_t) - \nabla_{\tilde{\mathbf{w}}} f_{\text{LH}}(g^* \mathbf{w}'_t)\|^2 \\ &\stackrel{(53)}{\leq} \zeta \|\mathbf{w}'_t\|^2 \|a_t^{(T_s)} \mathbf{w}'_t - g^* \mathbf{w}'_t\|^2 \\ &\leq \zeta \|\mathbf{w}'_t\|^4 (a_t^{(T_s)} - g^*)^2 \\ &\leq \zeta \|\mathbf{w}_t\|^4 \|\mathbf{w}_t\|_{\mathbf{S}}^{-4} (a_t^{(T_s)} - g^*)^2 \\ &\stackrel{(2)}{\leq} \zeta \mu^{-2} (a_t^{(T_s)} - g^*)^2, \end{aligned} \quad (66)$$

where the last inequality is due to Assumption 1.

Combining (65) and (66) directly yields

$$\left(\partial_g f_{\text{LH}}(\mathbf{w}_t, a_t^{(T_s)})\right)^2 \leq 2^{-T_s} \zeta |b_t^{(0)} - a_t^{(0)}| / \mu^2, \quad (67)$$

which proves the assertion. \square

B.3.4 Directional convergence

Lemma 6 (Directional convergence). *Let all assumptions of Theorem 4 hold. Then, in each iteration $t \in \mathbb{N}^+$ of GDNP (Algorithm 1) with the following stepsize choice*

$$s_t = -\|\mathbf{w}_t\|_{\mathbf{S}}^3 / (L g_t \mathbf{E}_{\mathbf{z}} [\varphi'(g_t \mathbf{z}^\top \mathbf{w}_t / \|\mathbf{w}_t\|_{\mathbf{S}})] \mathbf{u}^\top \mathbf{w}_t), \quad t = 1, \dots, T_d$$

the norm of the gradient w.r.t. \mathbf{w} of f_{LH} as in Eq. (56) converges at the following linear rate

$$\|\mathbf{w}_t\|_{\mathbf{S}}^2 \|\nabla_{\mathbf{w}} f_{\text{LH}}(\mathbf{w}_t, g_t)\|_{\mathbf{S}^{-1}}^2 \leq (1 - \mu/L)^{2t} \Phi^2 g_t^2 (\rho(\mathbf{w}_0) - \rho^*).$$

Proof. The key insight for this proof is a rather subtle connection between the gradient of the reparametrized least squares objective (Eq. (8)) and the directional gradient of the learning halfspace problem (Eq. (56)):

$$\begin{aligned} \nabla_{\mathbf{w}} f_{\text{LH}}(\mathbf{w}, g) &\stackrel{(63)}{=} g c_1(\mathbf{w}, g) \mathbf{A}_{\mathbf{w}} \mathbf{u} \\ &= g c_1(\mathbf{w}, g) \left(\mathbf{u} - \left(\frac{\mathbf{w}^\top \mathbf{u}}{\|\mathbf{w}\|_{\mathbf{S}}^2} \right) \mathbf{S} \mathbf{w} \right) / \|\mathbf{w}\|_{\mathbf{S}} \\ &= g \frac{c_1(\mathbf{w}, g)}{\mathbf{u}^\top \mathbf{w}} \left(\mathbf{u}^\top \mathbf{w} \mathbf{u} - \frac{(\mathbf{w}^\top \mathbf{u})^2}{\|\mathbf{w}\|_{\mathbf{S}}^2} \mathbf{S} \mathbf{w} \right) / \|\mathbf{w}\|_{\mathbf{S}} \\ &= g \frac{c_1(\mathbf{w}, g) \|\mathbf{w}\|_{\mathbf{S}}}{\mathbf{u}^\top \mathbf{w}} (\mathbf{B} \mathbf{w}_t + \rho(\mathbf{w}) \mathbf{S} \mathbf{w}) / \|\mathbf{w}\|_{\mathbf{S}}^2 \\ &\stackrel{(18)}{=} -g \left(\frac{c_1(\mathbf{w}, g) \|\mathbf{w}\|_{\mathbf{S}}}{2 \mathbf{u}^\top \mathbf{w}} \right) \nabla_{\mathbf{w}} \rho(\mathbf{w}). \end{aligned} \quad (68)$$

Therefore, the directional gradients $\nabla_{\mathbf{w}}\rho(\mathbf{w})$ and $\nabla_{\mathbf{w}}f_{\text{LH}}(\mathbf{w}, g)$ align in the same direction for all $\mathbf{w} \in \mathbb{R}^d \setminus \{\mathbf{0}\}$. Based on this observation, we propose a stepsize schedule for GDNP such that we can exploit the convergence result established for least squares in Theorem 1. The iterates $\{\mathbf{w}_t\}_{t \in \mathbb{N}^+}$ of GDNP on f_{LH} can be written as

$$\begin{aligned} \mathbf{w}_{t+1} &= \mathbf{w}_t - s_t \nabla_{\mathbf{w}} f_{\text{LH}}(\mathbf{w}_t, g) \\ &\stackrel{(68)}{=} \mathbf{w}_t + s_t \left(\frac{g_t c_1(\mathbf{w}_t, g_t) \|\mathbf{w}_t\|_{\mathbf{S}}}{2\mathbf{u}^\top \mathbf{w}_t} \right) \nabla_{\mathbf{w}} \rho(\mathbf{w}_t). \end{aligned} \quad (69)$$

The stepsize choice of Eq.(54) guarantees that

$$s_t c_1(\mathbf{w}_t, g_t) g_t \|\mathbf{w}_t\|_{\mathbf{S}} / (2\mathbf{u}^\top \mathbf{w}_t) = -\|\mathbf{w}_t\|_{\mathbf{S}}^4 / (2L(\mathbf{w}_t^\top \mathbf{u})^2) \stackrel{(19)}{=} -\eta_t.$$

Thus, Eq. (69) can be rewritten as

$$\mathbf{w}_{t+1} = \mathbf{w}_t - \eta_t \nabla_{\mathbf{w}} \rho(\mathbf{w}_t),$$

which exactly matches the GD iterate sequence of Eq. (9) on $\rho(\mathbf{w})$. At this point, we can invoke the result of Theorem 1 to establish the following convergence rate:

$$\begin{aligned} \|\mathbf{w}_t\|_{\mathbf{S}}^2 \|\nabla_{\mathbf{w}} f_{\text{LH}}(\mathbf{w}_t, g_t)\|_{\mathbf{S}^{-1}}^2 &\stackrel{(68)}{=} \|\mathbf{w}_t\|_{\mathbf{S}}^2 c_1^2(\mathbf{w}_t, g_t) g_t^2 \|\nabla_{\mathbf{w}} \rho(\mathbf{w}_t)\|_{\mathbf{S}^{-1}}^2 / (2(\mathbf{u}^\top \mathbf{w}_t) / \|\mathbf{w}_t\|_{\mathbf{S}})^2 \\ &\stackrel{(3)}{\leq} \Phi^2 \|\mathbf{w}_t\|_{\mathbf{S}}^2 g_t^2 \|\nabla_{\mathbf{w}} \rho(\mathbf{w}_t)\|_{\mathbf{S}^{-1}}^2 / (2(\mathbf{u}^\top \mathbf{w}_t) / \|\mathbf{w}_t\|_{\mathbf{S}})^2 \\ &\leq \Phi^2 \|\mathbf{w}_t\|_{\mathbf{S}}^2 g_t^2 \|\nabla_{\mathbf{w}} \rho(\mathbf{w}_t)\|_{\mathbf{S}^{-1}}^2 / |4\rho(\mathbf{w}_t)| \\ &\stackrel{(11)}{\leq} \Phi^2 g_t^2 (\rho(\mathbf{w}_t) - \rho^*) \\ &\stackrel{(10)}{\leq} (1 - \mu/L)^{2t} \Phi^2 g_t^2 (\rho(\mathbf{w}_0) - \rho^*). \end{aligned} \quad (70)$$

□

B.3.5 Combined convergence guarantee

Using Proposition 4 and combining the results obtained for optimizing the directional and scalar components, we finally obtain the following convergence guarantee:

$$\begin{aligned} \|\nabla_{\tilde{\mathbf{w}}} f_{\text{LH}}(\tilde{\mathbf{w}}_{T_d})\|_{\mathbf{S}^{-1}}^2 &\stackrel{(59)}{=} \|\mathbf{w}_{T_d}\|_{\mathbf{S}}^2 \|\nabla_{\mathbf{w}} f_{\text{LH}}(\mathbf{w}_{T_d}, g_{T_d})\|_{\mathbf{S}^{-1}}^2 / g_{T_d}^2 + (\partial_g f_{\text{LH}}(\mathbf{w}_{T_d}, g_{T_d}))^2 \\ &\stackrel{(70)}{\leq} (1 - \mu/L)^{2T_d} \Phi^2 (\rho(\mathbf{w}_0) - \rho^*) + (\partial_g f_{\text{LH}}(\mathbf{w}_{T_d}, g_{T_d}))^2 \\ &\stackrel{(67)}{\leq} (1 - \mu/L)^{2T_d} \Phi^2 (\rho(\mathbf{w}_0) - \rho^*) + 2^{-T_s} \zeta |b_{T_d}^{(0)} - a_{T_d}^{(0)}| / \mu^2. \end{aligned}$$

C Neural Networks

Recall the training objective of the one layer MLP presented in Section 5:

$$\min_{\tilde{\mathbf{W}}, \Theta} \left(f_{\text{NN}}(\tilde{\mathbf{W}}, \Theta) := \mathbf{E}_{y, \mathbf{x}} \left[\ell \left(-y F(\mathbf{x}, \tilde{\mathbf{W}}, \Theta) \right) \right] \right), \quad (\text{Revisited 15})$$

where

$$F(\mathbf{z}, \tilde{\mathbf{W}}, \Theta) := \sum_{i=1}^m \theta^{(i)} \varphi(\mathbf{z}^\top \tilde{\mathbf{w}}^{(i)}).$$

Algorithm 3 Bisection

```

1: Input:  $T_s, a_t^{(0)}, b_t^{(0)}, f$ 
2: for  $m = 0, \dots, T_s$  do
3:    $c = (a^{(m)} + b^{(m)})/2$ 
4:   if  $\partial_g f(c, \mathbf{w}_t) \cdot \partial_g f(a^{(m)}, \mathbf{w}_t) > 0$  then
5:      $a^{(m+1)} \leftarrow c$ 
6:   else
7:      $b^{(m+1)} \leftarrow c$ 
8:   end if
9: end for
10:  $g \leftarrow a^{(T_s)}$ 
11: return  $g$ 

```

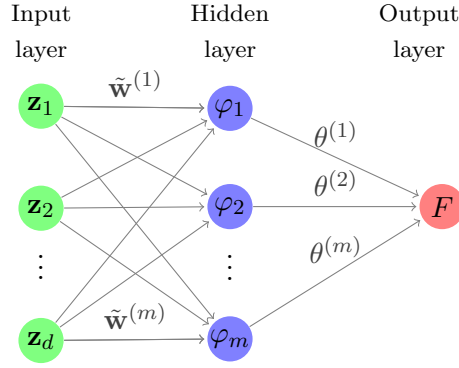


Figure 3: Neural network architecture considered in this paper.

Figure 3 illustrates the considered architecture in this paper.

Since the activation function is assumed to be an odd function (tanh), this choice allows us to equivalently rewrite the training objective as

$$\min_{\tilde{\mathbf{W}}, \Theta} \left(f_{\text{NN}}(\tilde{\mathbf{W}}, \Theta) = \mathbf{E}_{\mathbf{z}} \left[\ell(F(\mathbf{z}, \tilde{\mathbf{W}}, \Theta)) \right] \right). \quad (71)$$

By means of Assumption 2 and Stein's lemma (Eq. (52)) we can simplify the gradient w.r.t $\tilde{\mathbf{w}}_i$ as follows

$$\nabla_{\tilde{\mathbf{w}}^{(i)}} f_{\text{NN}}(\tilde{\mathbf{W}}, \Theta) / \theta^{(i)} = \mathbf{E}_{\mathbf{z}} \left[\ell^{(1)}(F(\mathbf{z}, \tilde{\mathbf{W}}, \Theta)) \varphi^{(1)}(\mathbf{z}^\top \tilde{\mathbf{w}}^{(i)} \mathbf{z}) \right] \quad (72)$$

$$= \alpha^{(i)} \mathbf{u} + \beta^{(i)} \mathbf{S} \tilde{\mathbf{w}}^{(i)} + \sum_{j=1}^m \gamma^{(i,j)} \mathbf{S} \tilde{\mathbf{w}}^{(j)}, \quad (73)$$

where the scalars $\alpha^{(i)}$, $\beta^{(i)}$ and $\gamma^{(i,j)}$ are defined as

$$\alpha^{(i)} := \mathbf{E}_{\mathbf{z}} \left[\ell^{(1)}(F(\mathbf{z}, \tilde{\mathbf{W}}, \Theta)) \varphi^{(1)}(\mathbf{z}^\top \tilde{\mathbf{w}}^{(i)}) \right] \quad (74)$$

$$\beta^{(i)} := \mathbf{E}_{\mathbf{z}} \left[\ell^{(1)}(F(\mathbf{z}, \tilde{\mathbf{W}}, \Theta)) \varphi^{(2)}(\mathbf{z}^\top \tilde{\mathbf{w}}^{(i)}) \right] \quad (75)$$

$$\gamma^{(i,j)} := \theta^{(j)} \mathbf{E}_{\mathbf{z}} \left[\ell^{(2)}(F(\mathbf{z}, \tilde{\mathbf{W}}, \Theta)) \varphi^{(1)}(\mathbf{z}^\top \tilde{\mathbf{w}}^{(i)}) \varphi^{(1)}(\mathbf{z}^\top \tilde{\mathbf{w}}^{(j)}) \right], \quad (76)$$

where $l^{(i)}(\cdot) \in \mathbb{R}$ and $\varphi^{(i)}(\cdot) \in \mathbb{R}$ represent the i -th derivative of $l(\cdot)$ and $\varphi(\cdot)$ with respect to their input (\cdot) .

C.1 Characterization of the objective

Interestingly, the normality assumption induces a particular global property on $f_{\text{NN}}(\tilde{\mathbf{W}})$. In fact, all critical weights $\hat{\mathbf{w}}_i$ align along one single line in \mathbb{R}^d , which only depends on *incoming* information into the hidden layer. This result is formalized in the next lemma.

Lemma 7. *Suppose Assumptions 1 and 2 hold and let $\hat{\mathbf{w}}^{(i)}$ be a critical point of $f_{\text{NN}}(\tilde{\mathbf{W}})$ with respect to hidden unit i and for a fixed $\Theta \neq \mathbf{0}$. Then, there exists a scalar $\hat{c}^{(i)} \in \mathbb{R}$ such that*

$$\hat{\mathbf{w}}^{(i)} = \hat{c}^{(i)} \mathbf{S}^{-1} \mathbf{u}, \quad \forall i = 1, \dots, m. \quad (77)$$

Proof. Recall the gradient of f_{NN} as given in Eq. (72). Computing a first order critical point requires setting the derivatives of all units to zero which amounts to solving the following system of non-linear equations:

$$\begin{aligned} (1) \quad & \alpha^{(1)} \mathbf{u} + \beta^{(1)} \mathbf{S} \hat{\mathbf{w}}^{(1)} + \sum_{j=1}^m \gamma^{(1,j)} \mathbf{S} \hat{\mathbf{w}}^{(j)} = 0 \\ (2) \quad & \alpha^{(2)} \mathbf{u} + \beta^{(2)} \mathbf{S} \hat{\mathbf{w}}^{(2)} + \sum_{j=1}^m \gamma^{(2,j)} \mathbf{S} \hat{\mathbf{w}}^{(j)} = 0 \\ & \vdots \\ (m) \quad & \alpha^{(m)} \mathbf{u} + \beta^{(m)} \mathbf{S} \hat{\mathbf{w}}^{(m)} + \sum_{j=1}^m \gamma^{(m,j)} \mathbf{S} \hat{\mathbf{w}}^{(j)} = 0, \end{aligned} \quad (78)$$

where each row (i) represents a system of d equations.

Matrix formulation of system of equations Let us rewrite (78) in matrix form. Towards this end, we define

$$\mathbf{U} = [\mathbf{u}, \mathbf{u}, \dots, \mathbf{u}] \in \mathbb{R}^{d \times m}, \quad \hat{\mathbf{w}} = [\hat{\mathbf{w}}^{(1)}, \hat{\mathbf{w}}^{(2)}, \dots, \hat{\mathbf{w}}^{(m)}] \in \mathbb{R}^{d \times m}$$

as well as

$$\mathbf{A} = \text{diag}(\alpha^{(1)}, \alpha^{(2)}, \dots, \alpha^{(m)}) \in \mathbb{R}^{m \times m}, \quad \mathbf{B} = \text{diag}(\beta^{(1)}, \beta^{(2)}, \dots, \beta^{(m)}) \in \mathbb{R}^{m \times m}$$

and

$$\mathbf{\Gamma} = \begin{bmatrix} \gamma^{(1,1)} & \gamma^{(1,2)} & \dots & \gamma^{(1,m)} \\ \gamma^{(2,1)} & \gamma^{(2,2)} & \dots & \gamma^{(2,m)} \\ & & \ddots & \\ \gamma^{(m,1)} & \gamma^{(m,2)} & \dots & \gamma^{(m,m)} \end{bmatrix}.$$

Note that $\mathbf{\Gamma} = \mathbf{\Gamma}^\top$ since $\gamma^{(i,j)} = \gamma^{(j,i)}, \forall i, j$.

Solving the system of equations Using the notation introduced above, we can write (78) as follows

$$\begin{aligned} \mathbf{U} \mathbf{A} + \mathbf{S} \hat{\mathbf{W}} \mathbf{B} + \mathbf{S} \hat{\mathbf{W}} \mathbf{\Gamma} &= \mathbf{0} \\ \Leftrightarrow \mathbf{S} \hat{\mathbf{W}} (\mathbf{B} + \mathbf{\Gamma}) &= -\mathbf{U} \mathbf{A} \\ \Leftrightarrow \hat{\mathbf{W}} &= -\mathbf{S}^{-1} \mathbf{U} \underbrace{\mathbf{A} (\mathbf{B} + \mathbf{\Gamma})^\dagger}_{:= \mathbf{D}}, \end{aligned} \quad (79)$$

where $(\mathbf{B} + \mathbf{\Gamma})^\dagger$ is the pseudo-inverse of $(\mathbf{B} + \mathbf{\Gamma})$.

As a result

$$[\hat{\mathbf{w}}^{(1)}, \hat{\mathbf{w}}^{(2)}, \dots, \hat{\mathbf{w}}^{(m)}] = -[\mathbf{S}^{-1} \mathbf{u}, \mathbf{S}^{-1} \mathbf{u}, \dots, \mathbf{S}^{-1} \mathbf{u}] [\mathbf{d}_1, \mathbf{d}_2, \dots, \mathbf{d}_m]$$

and hence the critical points of the objective are of the following type

$$\hat{\mathbf{w}}^{(i)} = -\mathbf{S}^{-1}\mathbf{U}\mathbf{d}_1 = -\left(\sum_{k=1}^m \mathbf{d}_i^{(k)}\right)\mathbf{S}^{-1}\mathbf{u}. \quad (80)$$

□

C.2 Possible implications for multilayer networks

From Eq. (77) in the last lemma we can conclude that the optimal direction of any $\hat{\mathbf{w}}^{(i)}$ is independent of the corresponding output weight $\theta^{(i)}$, which only affects $\hat{\mathbf{w}}^{(i)}$ through the scaling parameter $\hat{c}^{(i)}$. This is a very appealing property: Take a multilayer network and assume (for the moment) that all layer inputs are Gaussian. Then, Lemma 7 still holds for any given hidden layer and gives rise to a decoupling of the optimal direction of this layer with all downstream weights, which in turn simplifies the curvature structure of the network since many Hessian blocks become zero.

However, classical local optimizers such as GD optimize both, direction and scaling, at the same time and are therefore blind to the above global property. It is thus very natural that performing optimization in the reparametrized weight space can in fact benefit from splitting the subtasks of optimizing scaling and direction in two parts, since updates in the latter are no longer sensitive to changes in the downstream part of the network. In the next section, we theoretically prove that such a decoupling accelerates optimization of weights of each individual unit in the presence of Gaussian inputs. Of course, the normality assumption is very strong but remarkably the experimental results of Section 5.3 suggest the validity of this result beyond the Gaussian design setting and thus motivate future research in this direction.

C.3 Convergence analysis

Here, we prove the convergence result restated below.

Theorem 3. *[Convergence of GDNP on MLP] Suppose Assumptions 1–4 hold. We consider optimizing the weights $(\mathbf{w}^{(i)}, g^{(i)})$ of unit i , assuming that all directions $\{\mathbf{w}^{(j)}\}_{j < i}$ are critical points of f_{NN} and $\mathbf{w}^k = \mathbf{0}$ for $k > i$. Then, GDNP with step-size policy $s^{(i)}$ as in (85) and stopping criterion $h^{(i)}$ as in (86) yields a linear convergence rate on $f^{(i)}$ in the sense that*

$$\|\nabla_{\tilde{\mathbf{w}}^{(i)}} f(\tilde{\mathbf{w}}_t^{(i)})\|_{\mathbf{S}^{-1}}^2 \leq (1 - \mu/L)^{2t} C (\rho(\mathbf{w}_0) - \rho^*) + 2^{-T_s^{(i)}} \zeta |b_t^{(0)} - a_t^{(0)}|/\mu^2, \quad (16)$$

where the constant $C > 0$ is defined in Eq. (89).

Proof. According to the result of Lemma 7, all critical points of f_{NN} are aligned along the same direction as the solution of normalized least-squares. This property is similar to the objective of learning halfspaces (with Gaussian inputs) and the proof technique below therefore follows similar steps to the convergence proof of Theorem 4.

Gradient in the original parameterization Recall the gradient of f_{NN} is defined as

$$\nabla_{\tilde{\mathbf{w}}^{(i)}} f^{(i)}/\theta^{(i)} = \alpha^{(i)}\mathbf{u} + \beta^{(i)}\mathbf{S}\tilde{\mathbf{w}}^{(i)} + \sum_{j=1}^m \gamma^{(i,j)}\mathbf{S}\tilde{\mathbf{w}}^{(j)}. \quad (72 \text{ revisited})$$

Gradient in the normalized parameterization: Let us now consider the gradient of f_{NN} w.r.t the normalized weights, which relates to the gradient in the original parameterization in the following way

$$\nabla_{\mathbf{w}} f(\mathbf{w}, g) = g\mathbf{A}_{\mathbf{w}}\nabla_{\tilde{\mathbf{w}}} f(\tilde{\mathbf{w}}), \quad \partial_g f(\mathbf{w}, g) = \mathbf{w}^\top \nabla_{\tilde{\mathbf{w}}} f(\tilde{\mathbf{w}})/\|\mathbf{w}\|_{\mathbf{S}} \quad (57 \text{ revisited})$$

Replacing the expression given in Eq. (72) into the above formula yields

$$\nabla_{\mathbf{w}^{(i)}} f_{\text{NN}}/(g^{(i)}\theta^{(i)}) = \alpha^{(i)} \mathbf{A}_{\mathbf{w}^{(i)}} \mathbf{u} + \beta^{(i)} \mathbf{A}_{\mathbf{w}^{(i)}} \mathbf{S} \mathbf{w}^{(i)} + \sum_{j=1}^m \gamma^{(i,j)} \mathbf{A}_{\mathbf{w}^{(i)}} \mathbf{S} \mathbf{w}^{(j)}, \quad (81)$$

$$\mathbf{A}_{\mathbf{w}^{(i)}} := \mathbf{I}/\|\mathbf{w}^{(i)}\|_{\mathbf{S}} - \mathbf{S} \mathbf{w}^{(i)} \otimes \mathbf{w}^{(i)} / \|\mathbf{w}^{(i)}\|_{\mathbf{S}}^3. \quad (82)$$

Note that the constants $\alpha^{(i)}$, $\beta^{(i)}$ and $\gamma^{(i,j)}$ all depend on the parameters $\mathbf{w}^{(i)}$ and $\theta^{(j)}$ of the respective units i and j . The orthogonality of $\mathbf{S} \mathbf{w}^{(i)}$ to $\mathbf{A}_{\mathbf{w}^{(i)}}$ (see Eq. (58)) allows us to simplify things further:

$$\nabla_{\mathbf{w}^{(i)}} f_{\text{NN}}/(g^{(i)}\theta^{(i)}) = \alpha^{(i)} \mathbf{A}_{\mathbf{w}^{(i)}} \mathbf{u} + \sum_{j \neq i} \gamma^{(i,j)} \mathbf{A}_{\mathbf{w}^{(i)}} \mathbf{S} \mathbf{w}^{(j)} \quad (83)$$

We now use the initialization of weights $\{\mathbf{w}^{(k)} = c_k \mathbf{S}^{-1} \mathbf{u}\}_{k < i}$ and $\{\mathbf{w}^{(j)} = \mathbf{0}\}_{j > i}$ into the above expression to get

$$\begin{aligned} \nabla_{\mathbf{w}^{(i)}} f_{\text{NN}} &= \theta^{(i)} g^{(i)} \xi_t \mathbf{A}_{\mathbf{w}^{(i)}} \mathbf{u}, \quad \xi = \alpha^{(i)} + \sum_{j < i} \gamma^{(i,j)} c_j \\ &= \theta^{(i)} g^{(i)} \xi \left(\|\mathbf{w}^{(i)}\|_{\mathbf{S}} / (2 \mathbf{u}^\top \mathbf{w}^{(i)}) \right) \nabla \rho(\mathbf{w}^{(i)}) \end{aligned} \quad (84)$$

where $\nabla \rho(\mathbf{w})$ is the gradient of the normalized ordinary least squares problem (Eq. (8)), i.e.

$$-\nabla \rho(\mathbf{w})/2 = \left(\mathbf{u} \mathbf{u}^\top \mathbf{w} + \frac{(\mathbf{u}^\top \mathbf{w})^2}{\|\mathbf{w}\|_{\mathbf{S}}^2} \mathbf{S} \mathbf{w} \right) / \|\mathbf{w}\|_{\mathbf{S}}^2.$$

We conclude that the global characterization property described in Eq. (77) transfers to the gradient since the above gradient aligns with the gradient of $\rho(\mathbf{w})$.

Choice of stepsize and stopping criterion We follow the same approach used in the proof for learning halfspaces and choose a stepsize to ensure that the gradient steps on $f_{\text{NN}}^{(i)}$ match the gradient iterates on ρ , i.e.

$$\mathbf{w}_{t+1}^{(i)} = \mathbf{w}_t^{(i)} - s_t^{(i)} \theta^{(i)} g_t^{(i)} \xi_t \left(\|\mathbf{w}_t^{(i)}\|_{\mathbf{S}} / (2 \mathbf{u}^\top \mathbf{w}_t^{(i)}) \right) \nabla \rho(\mathbf{w}_t^{(i)}) = \mathbf{w}_t^{(i)} - \frac{\|\mathbf{w}_t^{(i)}\|_{\mathbf{S}}^2}{2L|\rho(\mathbf{w}_t^{(i)})|} \nabla \rho(\mathbf{w}_t^{(i)}),$$

which leads to the following choice of stepsize

$$s_t^{(i)} = \|\mathbf{w}_t^{(i)}\|_{\mathbf{S}}^3 / (L \theta^{(i)} g_t^{(i)} \xi_t \mathbf{u}^\top \mathbf{w}_t^{(i)}), \quad \xi_t = \alpha_t^{(i)} + \sum_{j < i} \gamma_t^{(i,j)} c_j. \quad (85)$$

If $\xi_t = 0$, then the gradient is zero. Therefore, we choose the stopping criterion as follows

$$h_t^{(i)} = \xi_t = \alpha_t^{(i)} + \sum_{j < i} \gamma_t^{(i,j)} c_j. \quad (86)$$

Gradient norm decomposition Proposition 4 relates the \mathbf{S}^{-1} -norm of the gradient in the original space to the normalized space as follows

$$\|\nabla_{\tilde{\mathbf{w}}^{(i)}} f(\tilde{\mathbf{w}}_t^{(i)})\|_{\mathbf{S}^{-1}}^2 = \|\mathbf{w}_t^{(i)}\|_{\mathbf{S}}^2 \|\nabla_{\mathbf{w}^{(i)}} f(\mathbf{w}_t^{(i)}, g^{(i)})\|_{\mathbf{S}^{-1}}^2 / (g_t^{(i)})^2 + \left(\partial_{g^{(i)}} f(\mathbf{w}_t^{(i)}, g_t^{(i)}) \right)^2. \quad (59 \text{ revisited})$$

In the following, we will establish convergence individually in terms of g and \mathbf{w} and then use the above result to get a global result.

Convergence in scalar $g^{(i)}$ Since the smoothness property defined in Assumption 4 also holds for $f_{\text{NN}}^{(i)}$, we can directly invoke the result of Lemma 5 to establish a convergence rate for g :

$$\left(\partial_{g^{(i)}} f^{(i)}(\mathbf{w}_t^{(i)}, g_{T_s}^{(i)}) \right)^2 \leq 2^{-T_s^{(i)}} \zeta |b_t^{(0)} - a_t^{(0)}| / \mu^2 \quad (67 \text{ revisited})$$

Directional convergence By the choice of stepsize in Eq. (85), the gradient trajectory on f_{NN} reduces to the gradient trajectory on $\rho(\mathbf{w})$. Hence, we can establish a linear convergence in $\mathbf{w}^{(i)}$ by a simple modification of Eq. (70):

$$\|\mathbf{w}_t^{(i)}\|_{\mathbf{S}}^2 \|\nabla_{\mathbf{w}} f^{(i)}(\mathbf{w}_t^{(i)}, g_t^{(i)})\|_{\mathbf{S}^{-1}}^2 \leq (1 - \mu/L)^{2t} \xi_t^2 g_t^2 (\rho(\mathbf{w}_0) - \rho(\mathbf{w}^*)). \quad (87)$$

The assumption 3 on loss with the choice of activation function as tanh allows us to bound the scalar ξ_t^2 :

$$\xi_t^2 \leq 2\Phi^2 + 2i \sum_{j < i} (\theta^{(j)} c_j)^2. \quad (88)$$

Combined convergence bound Combining the above results concludes the proof in the following way

$$\|\nabla_{\tilde{\mathbf{w}}^{(i)}} f(\tilde{\mathbf{w}}_t^{(i)})\|_{\mathbf{S}^{-1}}^2 \leq (1 - \mu/L)^{2t} C (\rho(\mathbf{w}_0) - \rho^*) + 2^{-T_s^{(i)}} \zeta |b_t^{(0)} - a_t^{(0)}| / \mu^2,$$

where

$$C = 2\Phi^2 + 2i \sum_{j < i} (\theta^{(j)} c_j)^2 > 0. \quad (89)$$

□

C.3.1 Asymptotic optimality on normalized weights

The linear convergence on unit i established in the last section requires the "above" weights $\{\mathbf{w}^{(j)}\}_{j < i}$ to be critical points of f_{NN} . In the next lemma, we prove that this condition holds asymptotically (when the number of iterations T_d and T_s go to ∞).

Lemma 2. *Consider $\mathbf{W}_{/i} := \{\mathbf{w}^{(j)}\}_{j < i} \cup \{\mathbf{w}^{(k)} = \mathbf{0}\}_{k > i}$ in Algorithm 2. Then $\mathbf{w}^{(j)}$ are critical points of f_{NN} for $j < i$ and $(T_d^{(j)}, T_s^{(j)}) \rightarrow (\infty, \infty)$.*

Proof. We use a proof by induction. For $i = 1$, the condition naturally holds as $\mathbf{W}_{/1} = \mathbf{0}$ in Algorithm 2. Suppose that condition holds $\mathbf{W}_{/i}$ for i , then Lemma 3 implies that $\mathbf{w}^{(i)}$ converges linearly to a critical point of f_{NN} . Now we prove that the weights $\{\mathbf{w}^{(j)}\}_{j < i}$ remain critical points of f_{NN} after having optimized $\mathbf{w}^{(i)}$. If $\mathbf{w}^{(i)}$ is a critical point of f_{NN} , then Lemma 3 implies that $\mathbf{w}^{(i)} = c_i \mathbf{S}^{-1} \mathbf{u}$. We first show that $\mathbf{A}_{\mathbf{w}^{(i)}} \mathbf{u} = \mathbf{0}$ (where $\mathbf{A}_{\mathbf{w}^{(i)}}$ is defined in Eq. (82)):

$$\mathbf{A}_{\mathbf{w}^{(i)}} \mathbf{u} = c_i (\|\mathbf{u}\|_{\mathbf{S}^{-1}}^{-1} - \|\mathbf{u}\|_{\mathbf{S}^{-1}}) \mathbf{u} = 0. \quad (90)$$

Since $\{\mathbf{w}^{(k)} = c_k \mathbf{S}^{-1} \mathbf{u}\}_{k \leq i}$ are critical points, we can prove that the gradient of any $\mathbf{w}^{(j)}$ is zero as

$$\nabla_{\mathbf{w}^{(j)}} f_{\text{NN}} = \alpha^{(j)} \mathbf{A}_{\mathbf{w}^{(j)}} \mathbf{u} + \sum_{j \leq i} \gamma^{(i,j)} \mathbf{A}_{\mathbf{w}^{(j)}} \mathbf{S} \mathbf{w}^{(j)} \quad (91)$$

$$= \alpha^{(j)} \mathbf{A}_{\mathbf{w}^{(j)}} \mathbf{u} + \sum_{k \leq i} \gamma^{(j,k)} \mathbf{A}_{\mathbf{w}^{(j)}} \mathbf{u} \stackrel{(90)}{=} 0 \quad (92)$$

Therefore, $\mathbf{W}_{/(i+1)}$ fulfills the desired property and we can conclude the proof by mathematical induction. □

D Experimental Details

D.1 Learning Halfspaces

Setting We consider empirical risk minimization (ERM) as a surrogate for (12) in the binary classification setting and make two different choices for $\varphi(\cdot)$:

$$\text{softplus}(\mathbf{w}^\top \mathbf{z}) := \mathbf{E}_{\mathbf{z}} [\log(1 + \exp(\tilde{\mathbf{w}}^\top \mathbf{z}))] \text{ and } \text{sigmoid}(\mathbf{w}^\top \mathbf{z}) := 1/(1 + \exp(-\tilde{\mathbf{w}}^\top \mathbf{z})).$$

The first resembles classical convex logistic regression when $\mathbf{y}_i \in \{-1, 1\}$. The second is a commonly used non-convex, continuous approximation of the zero-one loss in learning halfspaces [31]

As datasets we use the common realworld dataset *a9a* ($n = 32'561, d = 123$) as well a synthetic data set drawn from a multivariate gaussian distribution such that $\mathbf{z} \sim \mathcal{N}(\mathbf{u}, \mathbf{S})$ ($n = 1'000, d = 50$).

Methods We compare the convergence behavior of GD and Accelerated Gradient Descent (AGD) [24] to three versions of GD in normalized coordinates. Namely, we assess (i) GDNP as stated in Algorithm 1, (ii) a simpler version, BN, which simultaneously updates \mathbf{w} and \mathbf{g} with one GD step on each parameter and (iii) Weight Normalization (WN) as presented in [27]. All methods use full batch sizes.

GDNP uses stepsizes according to the policy propose in Theorem 4. On the softplus, GD, AGD, WN and BN are run with their own, constant, grid-searched stepsizes. Weight- and Batch Norm use a different stepsize for direction and scaling but only take one gradient step in each parameter per iteration. Since the sigmoid setting is non-convex and many different local minima and saddle points may be approached by the different algorithms in different runs, there exist no meaningful performance measure to gridsearch the stepsizes. We thus pick the inverse of the gradient Lipschitz constant ζ for all methods and all parameters, except GDNP. To estimate ζ , we compute $\zeta_{\text{sup}} := \|\mathbf{Z}^\top \mathbf{Z}\|_2 / 10 \geq \sum_i \varphi(\mathbf{w}^\top \mathbf{z}_i)^{(2)} \|\mathbf{Z}^\top \mathbf{Z}\|_2 / n$ where $\mathbf{Z} := [z_1, \dots, z_n]^\top \in \mathbb{R}^{n \times d}$ and $\varphi(\cdot)^{(2)} \leq 0.1$. After comparison with the largest eigenvalue of the Hessian at a couple of thousand different parameters $\tilde{\mathbf{w}}$ we found the bound to be pretty tight. Note that for GDNP, we use $L := \|\mathbf{Z}^\top \mathbf{Z}\|_2$ which can easily be computed as a pre-processing step and is, contrary to ζ , independent of \mathbf{w} . AGD computes the momentum parameter $\beta_t = (t-2)/(t+1)$ in the convex case and uses a (grid-searched) constant $\beta_t = \beta \in [0, 1]$ in the non-convex setting. We initialize randomly, i.e. $\tilde{\mathbf{w}}_0, \mathbf{w}_0 \sim \mathcal{N}(0, 1)$ and choose g_0 such that $\tilde{\mathbf{w}}_0 = g\mathbf{w}_0 / \|\mathbf{w}_0\|_{\mathbf{S}}$.

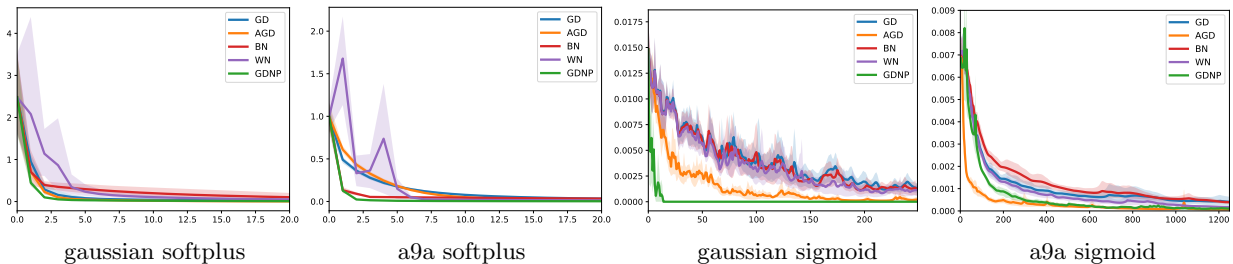


Figure 4: The plots are the same as in Figure 1 but show results in linear instead of log terms: Results of an average run (solid line) in terms of log suboptimality (softplus) and log gradient norm (sigmoid) over iterations as well as 90% confidence intervals of 10 runs with random initialization.

Interpretation

The gaussian design experiments clearly confirm Theorem 4 in the sense that the loss in the convex-, as well as the gradient norm in the non-convex case decrease at a linear rate. The results on *a9a* show that GDNP can accelerate optimization even when the normality assumption does not hold and in a setting where no covariate shift is present. This motivates future research of non-linear reparametrizations even in convex optimization.

Regarding BN and WN we found a clear trade-off between making fast progress in the beginning and optimizing the last couple of digits. In the above results of Figure 1 and 4 we report runs with stepsizes that were optimized for the latter case but we here note that early progress can easily be achieved in normalized parametrizations (which the linear *a9a* softplus plot actually confirms) e.g. by putting a higher learning rate on \mathbf{g} . In the long run similar performance to that of GD sets in, which suggests that the length-direction decoupling does not fully do the trick. The superior performance of GDNP points out that either an increased number of steps in the scaling factor g or an adaptive stepsize scheme such as the one given in Eq. (19) (or both) may significantly increase the performance of BN. It is an exciting open question whether similar

stepsize policies can be developed to speed up the training of Neural Networks. Finally, since GDNP performs similar to AGD in the non-gaussian setting, it is a logical next step to study how accelerated gradient methods like AGD or Heavy Ball perform in normalized coordinates.

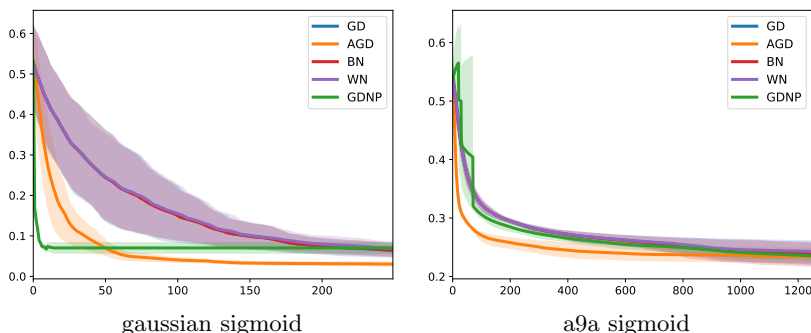


Figure 5: Addition to Figure 1 and 4: Suboptimality on the non-convex sigmoid problems in linear terms.

D.2 Neural networks

Setting and methods We test the validity of Theorem 3 and Lemma 7 outside the gaussian setting and for the simpler BN version by training two feedforward networks on the CIFAR10 image classification task. This dataset consists of 60000 32x32 images in 10 classes, with 6000 images per class [19]. The networks have six hidden layers with 50 hidden units in each of them. Each hidden unit has a *tanh* activation function, except for the very last layer which is linear. These scores are fed into a cross entropy loss layer which combines softmax and negative log likelihood loss. The experiments are implemented using the PyTorch framework [26].

The first network is trained by standard GD and the second by GD in normalized coordinates (i.e. BN) with the same fixed stepsize on \mathbf{w} and \mathbf{w} , but we increase the learning rate on \mathbf{g} by a factor of 10 which accelerates training significantly. We measure the cross-dependency of the central with all other layers in terms of the Frobenius norm of the second partial derivatives $\frac{\partial^2 f_{\text{NN}}}{\partial \mathbf{w}_4 \partial \mathbf{w}_i}$. This quantity signals how the gradients of layer 4 change when we alter the direction another layer. From an optimization perspective, this is a sound measure for the cross-dependencies since if it is close to zero (high), that means that a change in layer i induces no (a large) change in layer 4. Compared to gradient calculations, computing second derivatives is rather expensive $O(nd^2)$ (where $d = 50$), which is why we evaluate this measure every only 250 iterations.

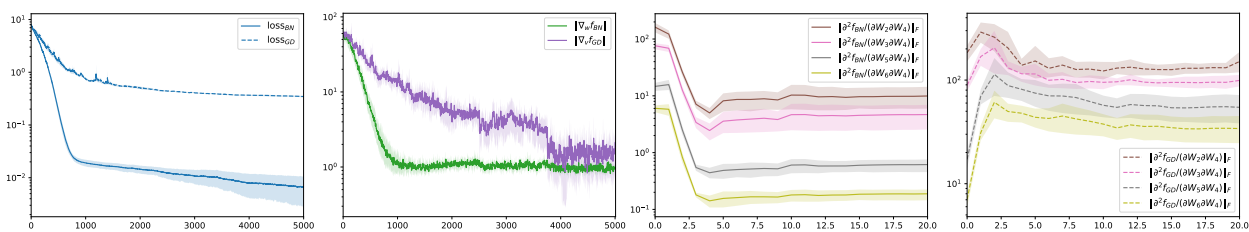


Figure 6: The plots are the same as in Figure 2 but show results in log instead of linear terms: (i) Loss, (ii) gradient norm and dependencies between central- and all other layers for BN (iii) and GD (iv) on a 6 hidden layer network with 50 units (each) on the CIFAR10 dataset.

Interpretation

Figure 2 and 6 confirm that the directional gradients of the central layer are affected far more by the upstream than by the downstream layers to a surprisingly large extent. Interestingly, this holds even before reaching a critical point. The cross-dependencies are generally decaying for BN while they remain elevated in the GD Network, which suggest that BN is able to exploit the length-direction decoupling to simplify the networks curvature structure in \mathbf{w} , which in turn simplifies the Gradient Descent trajectory in these coordinates for faster convergence. Of course, we cannot untangle this effect fully from the covariate shift reduction that was mentioned in the introduction. Yet, the fact that the (de-)coupling increases in the distance to the middle layer (note how earlier (later) layers are more (less) important for the \mathbf{W}_4) emphasizes the relevance of this analysis particularly for deep neural network structures, where downstream dependencies might vanish completely with depth. This does not only make gradient based training easier but also suggests the possibility of using partial second order information, such as diagonal Hessian approximations (e.g. proposed in [22]).